NJC

New Journal of Chemistry

A journal for new directions in chemistry

www.rsc.org/njc

Volume 36 | Number 3 | March 2012 | Pages 513–844

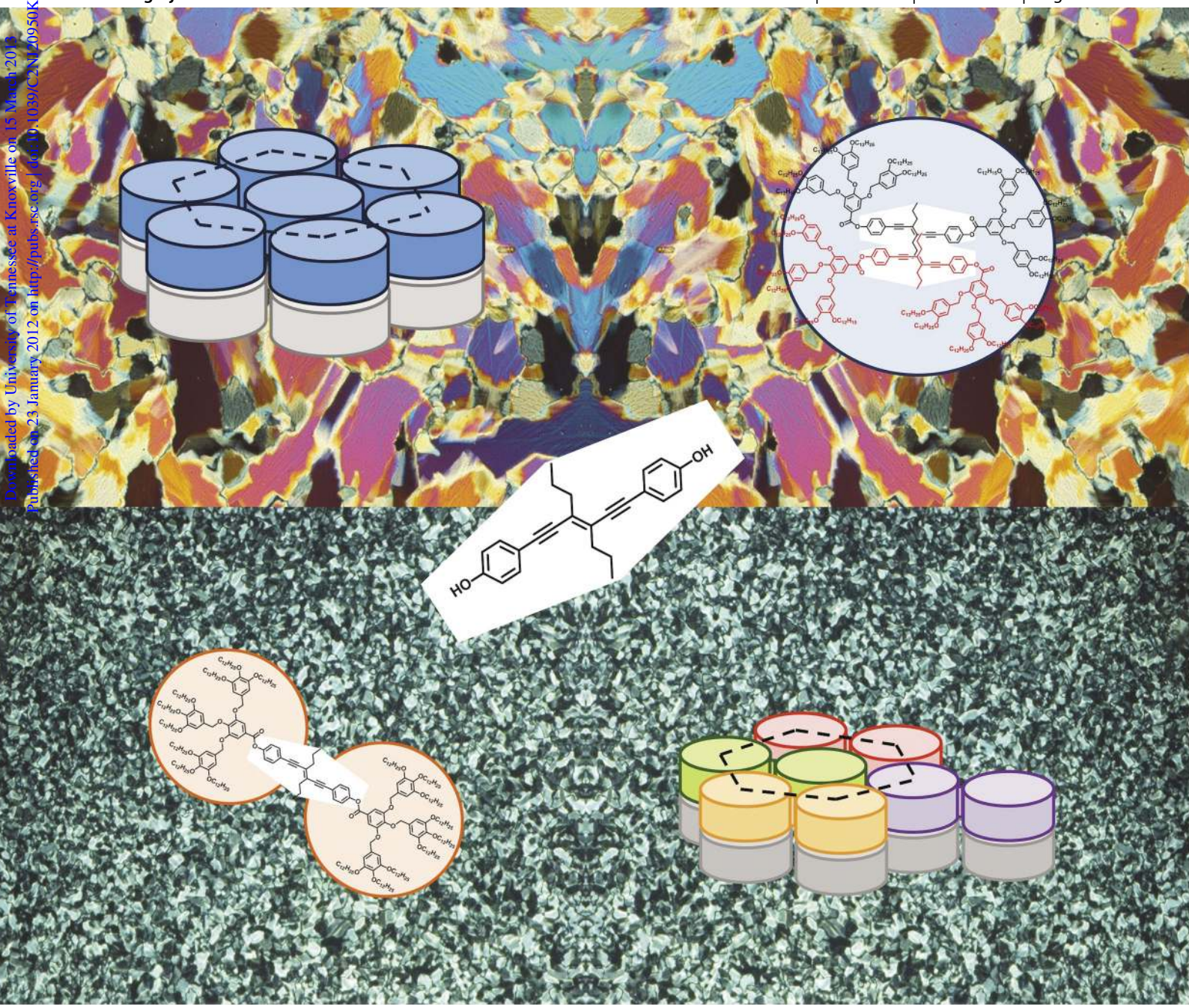

ISSN 1144-0546

RSC Publishing

cnrs

COVER ARTICLE

Sierra, Ballesteros *et al.*

A linear conjugated core for functional columnar liquid crystals

NJC

Dynamic Article Links
View Article Online

Cite this: *New J. Chem.*, 2012, **36**, 830–842

www.rsc.org/njc

PAPER

A linear conjugated core for functional columnar liquid crystals†

Ana Pérez,[a] José Luis Serrano,[a] Teresa Sierra,*[b] Alfredo Ballesteros,*[c] Diana de Saá,[c] Roberto Termine,[d] Upendra Kumar Pandey[d] and Attilio Golemme[d]

Received (in Montpellier, France) 10th November 2011, Accepted 6th January 2012
DOI: 10.1039/c2nj20950k

Two series of polycatenar molecules consisting of a π-conjugated rigid core derived from 3-hexen-1,5-diyne coupled to different types of benzoic acid derivatives have been prepared and their potential as multifunctional materials has been investigated. The size ratio between the rigid core and the benzoate-derived groups, which vary in bulk, is crucial to address self-organization, thus indicating the delicate balance of forces involved in liquid crystalline (LC) behaviour. LC nematic, crystalline or LC columnar behaviour is observed depending on the structure of the benzoate moiety. Hexagonal two-dimensional columnar organization is attained for mesogens with benzoate-derived groups bearing six and nine alkoxylic tails. The stacking unit of the columnar organizations is different depending on the total number of tails, twelve or eighteen, with two molecules and half a molecule per columnar stratum, respectively. Macroscopic properties related to molecular structure, such as luminescence, chirality and electroactivity, have also been studied. Luminescent behaviour is observed for all mesogenic materials, which show higher Stokes shifts than in solution. In addition, supramolecular chirality in the mesophase has been observed for a chiral mesogen. Finally, the photoconducting behaviour of two of the columnar materials has been evaluated.

Introduction

The design of multifunctional materials is one of the most interesting targets in materials chemistry. The combination of different physical properties in the same material may simplify the processing required to construct the corresponding devices and this aspect is of great importance in fields such as organic optoelectronics.[1] In an effort to achieve optoelectronic materials, a great deal of research effort has been focused on the supramolecular organization of the molecules.[2–6] The appropriate organization of the different functional building blocks in such a way that one or several properties are magnified, or the appearance of cooperative effects in the material due to the influence of the neighboring molecules, are ideal situations that must be considered for the development of high-performance functional materials.

In this respect, the combination of liquid crystalline order with other physical properties is particularly interesting to obtain multifunctional materials in which the control of the macroscopic molecular arrangement is essential for a certain property to manifest itself or to be enhanced, especially those properties that are direction-dependent.[7–9] Liquid crystals allow us to control order at the microscopic level and this can be extended to the macroscopic regime through appropriate processing and bulk alignment. Thus, for example, the effects of π-conjugation and organization on emission and conductive properties have led to an increasing interest for columnar liquid crystals as an approach to luminescent and semiconductor materials for optoelectronic applications.[10] Indeed, columnar phases of tailor-made mesogenic cores have been synthesized and investigated with regard to their application as semiconductors with high charge-carrier mobility values and intense fluorescence.[11]

The molecular design of columnar liquid crystals does not rely on disk-like structures only. Phasmidic or polycatenar liquid crystals are a family of thermotropic mesogens that are generally composed of a rod-like core and two half-disk-shaped units (aromatic end groups containing several flexible tails).[12] These mesogenic structures combine the structural and mesogenic properties of conventional calamitic and discotic liquid crystals. As a result, polycatenar liquid crystals not only display

[a] *Instituto de Nanociencia de Aragón, Química Orgánica, Facultad de Ciencias, Universidad de Zaragoza, 50009-Zaragoza, Spain*
[b] *Instituto de Ciencia de Materiales de Aragón, Química Orgánica, Facultad de Ciencias, Universidad de Zaragoza-C.S.I.C., 50009-Zaragoza, Spain. E-mail: tsierra@unizar.es*
[c] *Departamento de Química Orgánica e Inorgánica and Instituto Universitario de Química Organometálica "Enrique Moles", Unidad Asociada al C.S.I.C., Universidad de Oviedo, C/Julián Clavería, 8, 33006-Oviedo, Spain. E-mail: abg@uniovi.es*
[d] *Centro di Eccellenza CEMIF.CAL, LASCAMM CR-INSTM, CNR-IPCF UOS CS - LiCryL, Dipartimento di Chimica, Università della Calabria, 87036 Rende, Italy*

† Electronic supplementary information (ESI) available: Synthetic procedures and compounds analytical data. POM DSC, X-ray diffraction, UV-Vis, fluorescence, CD measurements, cyclic voltammetry. See DOI: 10.1039/c2nj20950k

conventional nematic and smectic mesophases, but they also commonly display columnar mesomorphism in which the composition of the stacking units is strongly dependent on the particular structure of the molecule. Furthermore, this approach allows tailoring of the mesogen design toward the achievement of functional liquid crystals with luminescent[13] and photoconducting properties suitable for optoelectronic purposes.[14]

In a previous communication, we described a new polycatenar mesogen (**C_3B9** in Chart 1) derived from a new core, 1,6-diphenyl-3,4-dipropyl-3-hexen-1,5-diyne (**C_3** in Chart 1).[15] This core has a rod-like shape, high electronic conjugation and fluorescence properties in solution, which make it interesting to implement functionality into liquid crystalline materials. The mesogenic compound, **C_3B9**, self-organized into a Col_h mesophase, which showed an unusual supramolecular organization with half a molecule constituting the stacking unit of the column. Furthermore, the new mesogen displayed luminescence in solution as well as in the mesophase.

On the basis of these results, we have explored the possibilities of tuning the mesomorphic behaviour of this π-conjugated core, and the effect of the resulting mesomorphic organization on the optic and electronic properties of the materials. In the present paper we report two conjugated cores, the previously reported, **C_3**, and the new one, **C_{10}**, derived from 1,6-diphenyl-3,4-didecyl-3-hexen-1,5-diyne (Chart 1).[16] These cores have been modified in the two terminal positions with different types of aromatic acid bearing long aliphatic chains: acids **A**, derived from benzoic acid, and acids **B**, derived from 3,4,5-tribenzyloxybenzoic acid. These carboxylate moieties contribute to the design of molecules, **CA** and **CB** (Chart 1), with structurally differentiated parts, which promote liquid crystalline order through nanosegregation. Accordingly, calamitic behaviour is observed for compounds derived from 4-dodecyloxybenzoic acid (**A1**), whereas columnar mesomorphism appears for derivatives with twelve (**C_nB6**) and eighteen (**C_nB9**) terminal chains. Moreover, the properties encoded in the molecule, *i.e.* chirality or electronic and luminescent features, are transferred to the resulting mesomorphic organization and hence manifested in the final material.

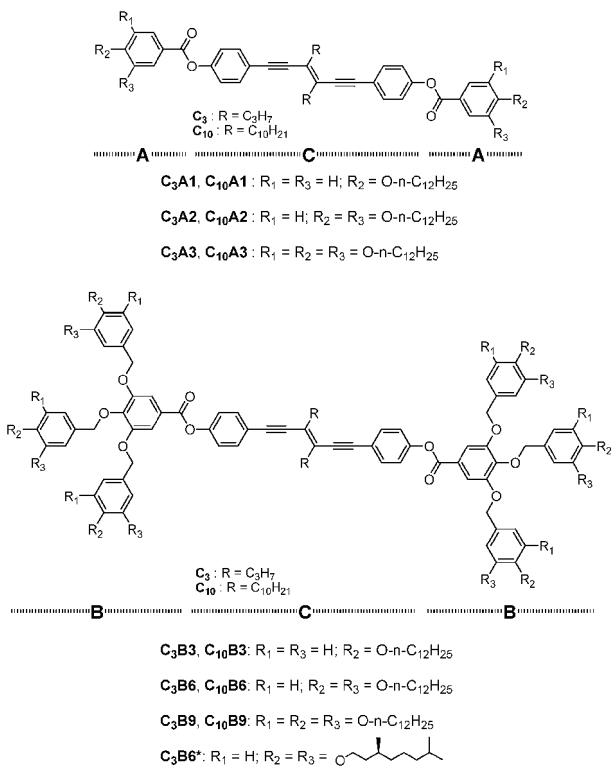

Chart 1 Chemical structure of the final compounds prepared by coupling the rigid π-conjugated core, **C**, with different benzoic acid derivatives (types **A** and **B**).

Results and discussion

Synthesis

The synthesis of the final compounds was carried out as outlined in Scheme 1. The synthetic and analytical details for the conjugated core **C_3**, with propyl groups as substituents in the central double bond, were described elsewhere.[15] The core **C_{10}**, with decyl groups as substituents in the central double bond, was prepared by following the same procedure as described for **C_3** (see ESI†).[16]

The benzoic acid derivatives **A1**, **A2** and **A3**, with one, two and three dodecyloxy chains, respectively, were prepared by Williamson etherification of the corresponding methyl hydroxybenzoate with the appropriate alkyl bromide followed by ester cleavage, as described elsewhere.[17] Likewise, the acids **B3**, **B6** and **B9** were prepared, as reported previously, by Williamson etherification of methyl 3,4,5-trihydroxybenzoate with the appropriate benzyl chloride, followed by ester cleavage.[18] Acid **B6*** is reported here for the first time (see ESI†) and was synthesized by following the same procedure as for acids **B3**, **B6** and **B9**.

Coupling of acid derivatives **A** and **B** with either **C_3** or **C_{10}** to give the target compounds was carried out by a double esterification reaction with DCC catalyzed by DMAP in dry dichloromethane (Scheme 1).

Thermal properties

The two conjugated cores, **C_3** and **C_{10}**, are crystalline materials. The length of the lateral chain has a marked influence on the melting point; compound **C_3**, bearing the shorter propyl group, has a higher melting temperature (172 °C) than compound **C_{10}** (with the longer decyl lateral group), which has a much lower melting point of 72 °C. As far as the mesogenic nature of the acids is concerned, all of them show liquid crystalline behavior apart from **A2** and **A3**. The mesophase characteristics have already been reported in the literature for acids **A1**, **B3** and **B9**. The mesophase of acid **B6** was identified as Col_h by POM and X-ray diffraction (see ESI†).[18b,19] Likewise, the chiral acid **B6*** shows a Col_h phase that is stable over a wide temperature range, including room temperature. To help the comparison between acids and their corresponding final compounds, the thermal behavior of all the acids is listed in Tables 1 and 2.

The thermal behaviour of the potential mesogens, **CA** and **CB**, was characterized by polarizing optical microscopy (POM) and differential scanning calorimetry (DSC). Phase transition temperatures and associated enthalpy values are summarized in Tables 1 and 2.

Rod-like compounds **C_3A1** and **C_{10}A1** showed nematic behaviour and, in a similar way to the respective **C_3** and **C_{10}** precursors, **C_3A1** has higher transition temperatures

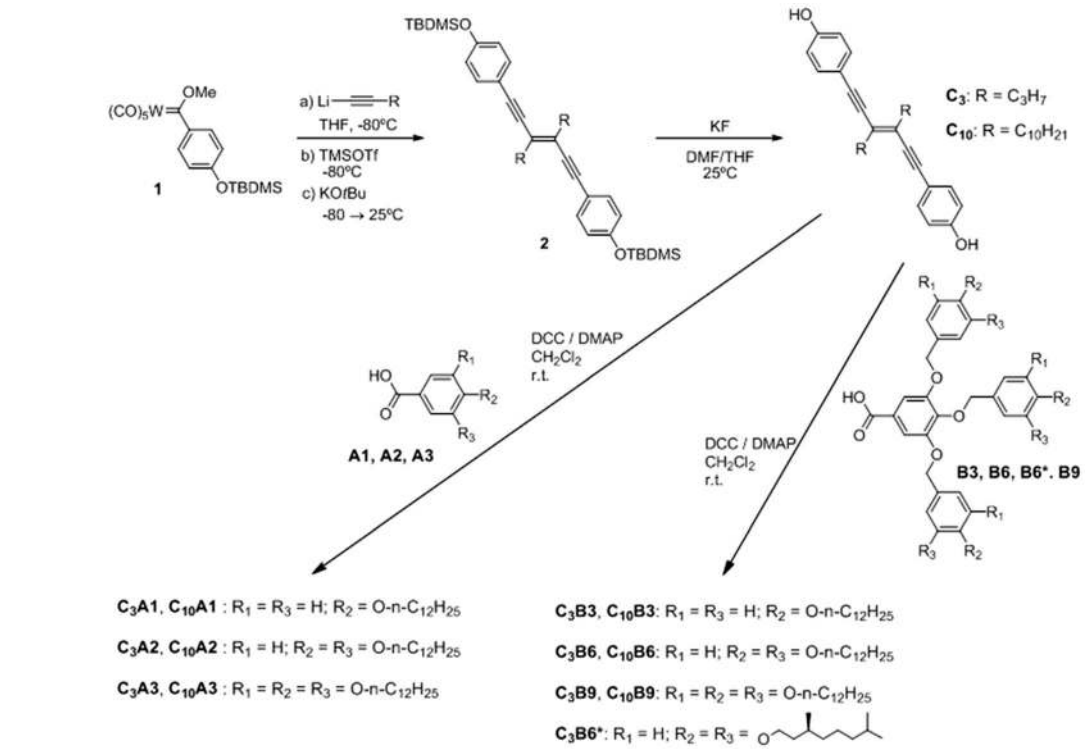

Scheme 1 Synthetic scheme followed to prepare the target compounds.

Table 1 Transition temperatures and associated enthalpy values of compounds **CA** and their acid precursors **A**, as determined by DSC

Compound	Transition temperatures[a]/°C [enthalpies/kJ mol^{-1}]								
A1[17]	Cr_1	32.1 [−10.8]	Cr_2	92.3 [39.3]	SmC	129.4 [1.9]	N	137.0 [2.4]	I
A2[17]	Cr_1	94.0 [8.7]	Cr_2	118.3 [58.4]					I
A3[17]	Cr	56.4 [62.6]							I
C_3A1	Cr	95.6 [71.4]					N	156.8 [3.0]	I
C_3A2	Cr	80.0 [87.8]							I
C_3A3	Cr	52.9 [112.0]							I
C_{10}A1	Cr	77.1 [61.8]					N	88.6 [1.7]	I
C_{10}A2	Cr	103.1 [122.1]							I
C_{10}A3	Cr_1	25.4 [72.8]	Cr_2	36.4 [−18.1]	Cr_3	50.2 [34.7]			I

Cr: crystalline phase, N: nematic mesophase, SmC: smectic C mesophase, I: isotropic liquid. [a] Reported are the onset values of transitions observed for the corresponding second scan at 10 °C min^{-1}.

Table 2 Transition temperatures and the associated enthalpy values of compounds **CB** and their acid precursors **B**, as determined by DSC

Compound	Transition temperatures[a]/°C [enthalpies/kJ mol^{-1}]								
B3[18b]	Cr	5.6 [17.3]					Col_h	136.8[b] [4.9]	I
B6	Cr	46.0 [3.7]					Col_h	132.6 [2.6]	I
B9[18b]	Cr_1	−13.1 [19.9]	Cr_2	18.1 [−94.6]	Cr_3	82.7 [109.5]	Cub	117.0 [3.8]	I
B6*							Col_h	89.6 [1.0]	I
C_3B3	Cr_1	25.6 [20.8]	Cr_2	76.3 [63.5]					I
C_3B6	M	8.1[b] [30.6]					Col_h	107.0 [29.7]	I
C_3B9			Col_h	40.3 [−84.2]	Cr	84.6 [149.8]	Col_h	59.6[d] [13.6]	I
C_3B6*							Col_h	58.3 [16.8]	I
C_{10}B3	Cr_1	46.1 [31.4]	Cr_2	85.9 [126.5]					I
C_{10}B6	M	7.9[b] [65.3]	Col_h	52.0 [−171.7]	Cr	92.1 [170.5]	Col_h	98.3 [29.9]	I
C_{10}B9	Cr	71.8 [199.2]					(Col_h	61[c,d])	I

Cr: crystalline phase, M: unidentified mesophase, Cub: cubic mesophase, Col_h: hexagonal columnar mesophase, I: isotropic liquid. [a] Reported are the onset values of transitions observed in the second heating–cooling cycle at 10 °C min^{-1}, except for (b), for which the maximum of the peak is given. [c] Transition temperature determined by POM. [d] Monotropic transition.

than **C_{10}A1**. Compound **C_3A1** shows a broad mesophase range in contrast to compound **C_{10}A1**, which has a nematic phase over a short temperature range. This difference is probably due to the greater steric hindrance of the decyl

lateral chains,[20] which hampers intermolecular interactions in **C_{10}A1** and lowers transition temperatures.

Compounds derived from acids **A2** or **A3**, with a phasmidic-like molecular shape, are not liquid crystalline. The increase in the number of terminal aliphatic chains prevents calamitic behaviour but their presence is not enough to favor a columnar arrangement in the mesophase.

In order to enhance molecular π-stacking by nanosegregation, we synthesized new compounds bearing bulky carboxylate groups, **B**. These dendritic moieties, firstly described by Percec, have been reported to show great self-organization potential.[21] Compounds derived from the acid **B3** do not exhibit liquid crystalline behaviour.

Compounds with terminal groups derived from acids **B6**, **B6*** and **B9** self-organize into columnar mesophases. **B6** and **B6*** derivatives show enantiotropic mesophases whereas **B9** derivatives show monotropic mesomorphism.

From data gathered in Table 2, it can be deduced that an optimum size-ratio between the bis-dendronized rigid π-conjugated core and the aliphatic regions (π-stacking and flexibility, respectively) exists, and this ensures stable mesomorphic properties. This is the case for compounds **C_3B6**, **C_{10}B6** and **C_3B6***. Compounds derived from acid **B6** show Col_h behaviour at room temperature. In addition, both derivatives, **C_3B6** (see ESI†) and **C_{10}B6**, show a mesophase below 8 °C that could not be identified. Upon investigation by POM, compound **C_{10}B6** showed a mosaic-like texture (Fig. 1) on cooling from the isotropic liquid and this remained during the cooling and heating processes, with color changes corresponding to transitions in the DSC thermograms (see Fig. 1 and ESI†). This compound shows a Col_h mesophase that appears twice during the heating cycle. Indeed, the enantiotropic Col_h mesophase, with a small temperature interval in the heating process, can be supercooled below room temperature. Nevertheless, the mesophase is thermodynamically metastable at room temperature since it crystallizes on heating at 40.3 °C (cold crystallization). DSC thermograms between different temperature limits showed that this behavior repeats at different scan temperature limits and the cold crystallization is only avoided when cooling around 70 °C and further heating.

Compound **C_3B6*** shows Col_h mesomorphism and this is stable at room temperature for long periods of time as confirmed by the thermograms recorded after several months.

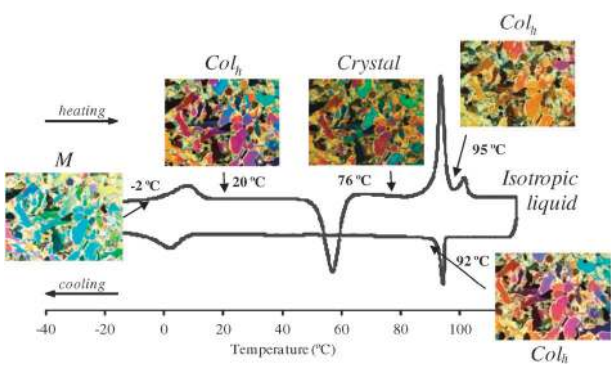

Fig. 1 Microphotographs (×20) of the textures observed for compound **C_{10}B6** at different temperatures, which correspond to different temperature ranges in the DSC thermogram (also shown). All of the photographs correspond to the same area of the sample.

Compounds derived from acid **B9**, **C_3B9** and **C_{10}B9**, show monotropic mesomorphic behavior. The Col_h mesophase of **C_3B9** was previously characterized,[15] although its data are herein included for the sake of comparison. The appearance of a Col_h mesophase for **C_{10}B9** could only be confirmed by POM. The textures displayed by both compounds are very similar, of the *schlieren*-type with low birefringence (see ESI†).

Structural characterization of the mesophases

All of the mesomorphic compounds were studied by X-ray diffraction with the aim of confirming the type of mesophase and determining the lattice parameters. Most of the experiments were performed at room temperature; however, in some cases high-temperature experiments were also carried out. The proposed indexing, lattice constants, and the observed and calculated maximum diffraction distances of the columnar mesophases are summarized in Tables 3 and 4. Table 3 collects the data of the acid precursors **B6** and **B6***. For **B6**, only a diffraction maximum is observed at low angles (see ESI†), which could not be enough to unambiguously confirm the hexagonal arrangement. However, the same result has been previously

Table 3 X-Ray diffraction data for the columnar mesophases of acids **B6** and **B6***

Compound	T/°C	Phase	Lattice constant/Å	d_{obs}/Å	d_{calc}/Å	hk
B6	90	Col_h	a = 40.3	34.9	34.9	10
				4.5 (br)		
B6*	24	Col_h	a = 35.9	30.5	31.1	10
				18.1	18.0	11
				16.0	15.6	20
				4.6 (br)		

br = broad.

Table 4 X-Ray diffraction data for the columnar mesophases of compounds **C_3B6**, **C_{10}B6**, **C_3B9** and **C_3B6***

Compound	T/°C	Phase	Lattice constant/Å	d_{obs}/Å	d_{calc}/Å	hk
C_3B6	24	Col_h	a = 54.1	47.1	46.9	10
				26.9	27.0	11
				4.4 (br)		
	79	Col_h	a = 52.9	45.4	45.8	10
				26.0	26.4	11
				23.0	22.9	20
				17.9	17.3	21
				4.5 (br)		
C_{10}B6	24	Col_h	a = 52.3	45.5	45.3	10
				26.2	26.1	11
				22.4	22.6	20
				4.4 (br)		
	96[a]	Col_h	a = 52.0	45.6	45.0	10
				26.0	26.0	11
				22.0	22.5	20
				4.5 (br)		
C_3B9	24	Col_h	a = 33.9	29.3	29.3	10
				4.4 (br)		
				3.9		
C_3B6*	24	Col_h	a = 47.7	41.6	41.3	10
				24.0	23.9	11
				20.3	20.7	20
				4.6 (br)		

[a] X-Ray diffractogram taken at 96 °C in the heating process and before reaching the isotropic liquid state.

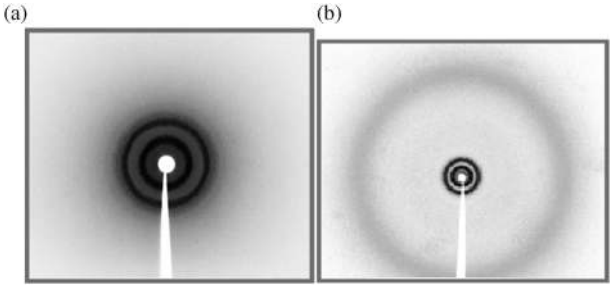

Fig. 2 (a) SAXS diagram corresponding to compound **C_3B6**, taken at 79 °C. (b) WAXS diagram taken at room temperature (24 °C) for compound **C_{10}B6**.

reported for other hexagonal columnar mesophases.[11g,17c,22] Moreover, the coherence of the lattice constants calculated for both compounds, given the different size of the alkoxylic tails, makes it reasonable to propose Col_h behavior for **B6**. Table 4 contains data for the final columnar materials, except **C_{10}B9** for which it was not possible to perform X-ray diffraction experiments because of its crystallization tendency after long experiment times.

The X-ray patterns for **C_3B6** and **C_{10}B6** are undoubtedly characteristic of a Col_h mesophase, both at RT and at high temperature. This was revealed by the presence of different sets of sharp low-angle maxima with a reciprocal spacing ratio $1:\sqrt{3}:\sqrt{4}:\sqrt{7}$, which can be assigned to the respective (10), (11), (20) and (21) reflections of a two-dimensional hexagonal lattice (Fig. 2 and ESI†). From the corresponding maxima, respective lattice parameters of 54.1 Å and 52.3 Å at room temperature were determined for both compounds. An outer broad halo was also observed corresponding to distances of approximately 4.4 Å, which was assigned to short-range correlation distances between aliphatic chains along the column. The variation of the *a* parameter with temperature was as expected, *i.e.* lower values were determined as the temperature increased since this change favours conformational freedom—especially for aliphatic chains. This result also supports that the Col_h mesophase of **C_{10}B6** is structurally the same at room temperature and upon crystallization and subsequent melting at 92.1 °C (see the ESI†).

If a density ρ close to 1 g cm^{-3} is supposed for these compounds, and estimating a periodic stacking of the molecular cores within a column of 4.4 Å, it is possible to deduce that there are two molecules per unit cell ($Z = 2$). In a hexagonal lattice there is one column per unit cell and this can be interpreted as two molecules forming each slice of the column (Fig. 3). The formation of columns consisting of two or more molecules per slice has already been described for other phasmidic-like mesogens.[14a-b,23]

This is in contrast to what we found for compound **C_3B9**.[15] The X-ray pattern for this compound contains only a single low-angle maximum and two wide-angle reflections. This pattern, together with POM observations, make us conclude that the compound self-organizes into a Col_h mesophase with a lattice parameter of 33.9 Å and a mean stacking distance of the cores along the column of 3.9 Å. These values allowed determining that there is half a molecule per unit cell ($Z = 0.5$), which corresponds to half a molecule per columnar stratum. Thus, the hexagonal two-dimensional network consists of

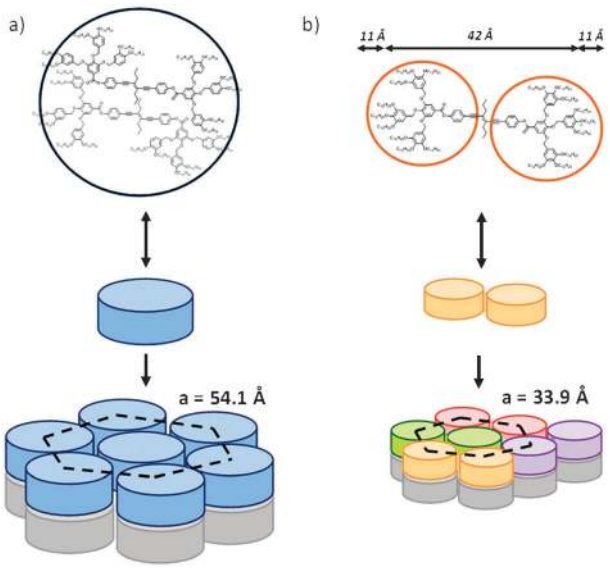

Fig. 3 Proposed models for the disposition of (a) two molecules per slice of the column in the columnar mesomorphic arrangement of compound **C_3B6**, and (b) half a molecule per slice of the column in the columnar mesomorphic arrangement of compound **C_3B9**. The size measured by stereomodels for the molecule is represented in (b). The length of the aliphatic part has been estimated considering an all-*trans* conformation for the chains.

columns interconnected two by two by the central core of some of the molecules. The lattice parameter is much smaller than the parameters of the Col_h mesophase found for compounds derived from acid **B6**, and this finding supports both models, the one proposed for **C_3B6** and **C_{10}B6** with $Z = 2$ and the one proposed for **C_3B9** with $Z = 0.5$ (Fig. 3).

Room temperature X-ray studies (Table 4) and density calculations confirmed that the behaviour of chiral compound **C_3B6*** is similar to that of its achiral analogues **C_3B6** and **C_{10}B6** and involves stacking of disk-like units formed by two molecules. The shorter hexagonal lattice constant *a* measured for **C_3B6*** compared to **C_3B6** is consistent with the smaller length and mass of the branched chain.

In summary, compounds derived from acids **A** show mesomorphic behaviour only for **A1** derivatives. Thus, **C_3A1** and **C_{10}A1**, which have a rod-like geometry, show a calamitic nematic mesophase. The lateral chain (propyl for the **C_3** derivative or decyl for the **C_{10}** derivative) affects intermolecular interactions. Accordingly, decrease of melting temperature and significant destabilization of the nematic mesophase occur on increasing the length of the lateral chain.

As for compounds derived from acids **B**, more than six terminal chains in the acid are required to promote mesomorphism. Compounds bearing twelve chains (**C_3B6**, **C_{10}B6** and **C_3B6***) show stable Col_h mesomorphic behavior in which two molecules form the cross section of the column. Compounds bearing 18 chains (**C_3B9** and **C_{10}B9**) also show Col_h liquid crystalline properties, but in this case the cross section of the column contains only half a molecule. In an effort to explain these observations, we propose that **B6** is more planar than acid **B9** and that π-stacking interactions are favored for the derivatives of the former system. In contrast, it may not be possible for all

of the chains in **B9** derivatives to be located within the same plane and stacking of molecules is therefore blocked (indeed, acid **B9** shows cubic mesomorphism interpreted by a conical shape).[18b] In this situation, the bulky moiety derived from acid **B9** can be better accommodated within the bay formed between two columns that are covalently linked by the conjugated core, thus favoring efficient filling of the space to stabilize the mesophase.

Chirooptical properties

To test the possibility of inducing supramolecular chirality into the columnar assembly of this type of compound,[24] we prepared compound **C_3B6*** in which the acid moiety bears six chiral tails derived from (*S*)-citronellol. The Col_h mesophase of this compound shows optical activity by circular dichroism (Fig. 4), which suggests that the chirality of the polycatenar phasmid-like molecules is transferred to the supramolecular organization.[25,26] The CD spectrum shown in Fig. 4 is the average of the spectra recorded upon rotation (in-plane) of the sample around the light beam every 60°. All the spectra were almost identical for all the orientations (see ESI†).[27] The CD spectrum shows a signal at the maximum of absorption of the chromophore that disappears upon heating the thin film above the clearing temperature of the mesophase. This situation is in contrast to the Col_h mesophase of the acid moiety, **B6***, which does not show circular dichroism signals despite the presence of chiral molecules. This finding can be interpreted in terms of the chiral supramolecular superstructure of **C_3B6*** being determined not only by the presence of stereogenic centers but also favoured by the π-stacking capability of the conjugated core **C_3** assisted by the tapered dendritic group, **B6***.

Luminescent properties

The luminescent properties of both series of compounds were investigated by absorption and emission spectroscopy in solution and, where applicable, in the mesophase.

Cores **C_3** and **C_{10}** were studied in THF solution (ESI†). Their absorption spectra show a maximum at 336 nm with a shoulder at around 360 nm. The emission properties of these two compounds are similar, with two maxima observed—a more intense one at 379 nm and a slightly weaker one at 397 nm. The corresponding quantum yields are included in Table 5. Excitation of crystalline thin films of **C_3** and **C_{10}** at 336 nm gave rise to extremely weak and noisy photoluminescence signals in the spectrofluorimeter. In fact, neither of these compounds is fluorescent to the naked eye when excited at 365 nm. **C_3** and **C_{10}** are indeed weak emitters in the solid state, probably due to emission quenching by "face-to-face" stacking, as deduced from the crystal structure of **C_3**.[15]

All final compounds, **CA** and **CB**, exhibit essentially the same absorption and emission profiles in solution and these are similar to those of the core **C** (Fig. 5). Upon excitation at 335 nm, all of the compounds show two maxima—a more intense one at 375 nm and a slightly weaker one at 397 nm. The fluorescence quantum yields of all the compounds were estimated from emission spectra in cyclohexane and in THF solutions, with 9,10-diphenylanthracene (Φ_{em} = 0.90 in

Table 5 Quantum yields calculated for all compounds in tetrahydrofuran and cyclohexane

	THF	Cy		THF	Cy
C_3	0.57	[a]	**C_{10}**	0.65	[a]
C_3A1	0.43	0.60	**C_{10}A1**	0.46	0.72
C_3A2	0.40	0.68	**C_{10}A2**	0.45	0.68
C_3A3	0.16	0.52	**C_{10}A3**	0.17	0.61
C_3B3	0.12	0.35	**C_{10}B3**	0.13	0.35
C_3B6	0.12	0.40	**C_{10}B6**	0.13	0.38
C_3B9	0.11	0.32	**C_{10}B9**	0.11	0.32
C_3B6*	0.12	0.33			

[a] Low solubility.

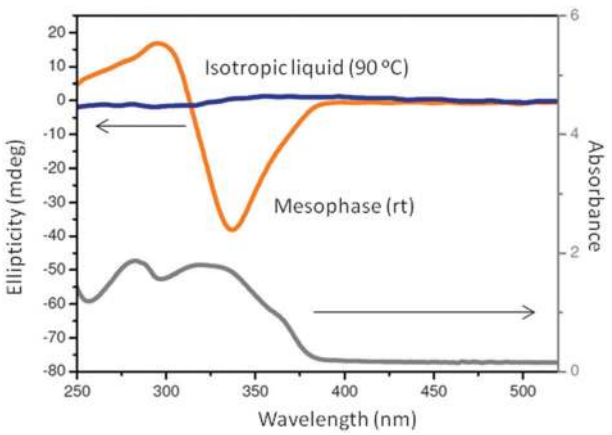

Fig. 4 Circular dichroism and absorption spectra of a thin film of **C_3B6***. Circular dichroism spectra were recorded in the isotropic phase at 90 °C and in the columnar mesophase at room temperature. The CD spectrum is the average of the spectra recorded upon rotation of the sample around the light beam every 60° in order to compensate for linear dichroism effects.

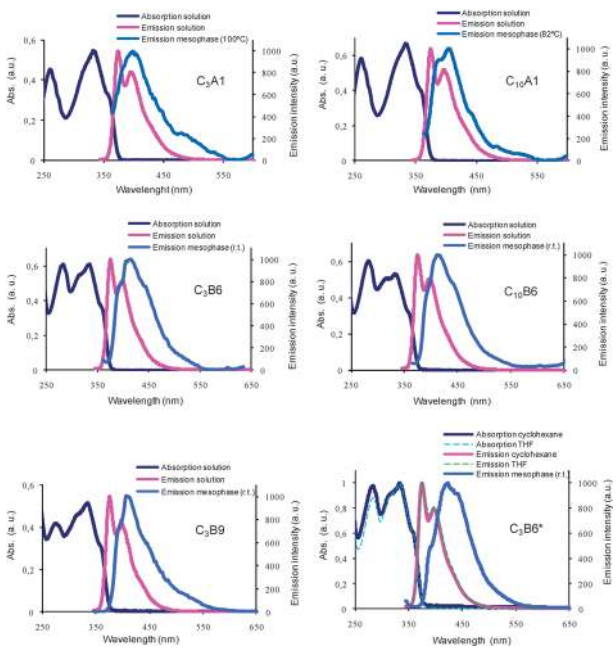

Fig. 5 Absorption and emission spectra of all the mesogenic compounds. Solution spectra correspond to cyclohexane solutions. For compound **C_3B6*** absorption and emission spectra corresponding to cyclohexane and THF solutions are presented to confirm that there is no difference in spectral profiles depending on the solvent.

cyclohexane) used as a standard.[28] The polarity of the solvent did not influence the absorption/emission spectrum profiles, but the fluorescence quantum yields were strongly dependent on the polarity of the solvent and also on the molecular structure (Table 5). Non-radiative processes, such as conformational changes or energy transfer, are less likely to occur in the apolar solvent (cyclohexane) than in the polar solvent (THF) and this results in higher quantum yields.[29] With respect to the influence of molecular structure, it is interesting to note that quantum yields are higher for compounds derived from acids **A** (Φ = 0.7–0.5) than for compounds derived from acids **B** (Φ = 0.4–0.3). Small acids **A** gave rise to compounds with luminescent properties in cyclohexane that are similar to those of the conjugated cores, $\mathbf{C_3}$ and $\mathbf{C_{10}}$. An overall decrease of quantum yields is observed on increasing the number of alkyloxy tails in the acid moiety. Electron-rich alkyloxy groups can act as fluorescence quenchers, probably through photo-induced electron-transfer processes.[11f,30] Bulky acids **B** gave rise to derivatives with lower quantum yields with respect to compounds derived from acids **A**. The reason may lie in the size of the carboxylate moiety, which makes the conjugated core **C** more predisposed to undergo distortions or conformational changes.[31]

All of the mesogenic compounds showed emission to the naked eye in their mesomorphic state. The emission spectra of calamitic compounds $\mathbf{C_3A1}$ and $\mathbf{C_{10}A1}$ were recorded at high temperatures of 100 °C and 82 °C, respectively (Fig. 5). The luminescence of compounds that show a columnar mesophase at room temperature was studied under ambient conditions (Fig. 5), except for compound $\mathbf{C_{10}B9}$, which crystallizes quickly at room temperature and could not be studied in the mesophase. In all cases, the absorption spectra in the mesophase (see Fig. 5 and ESI†) are essentially the same as those in solution but emission spectra obtained from mesomorphic thin films and from solution are quite different. Thin film spectra show only a single broad peak and this is red-shifted with respect to the solution emission maxima. Accordingly, Stokes shifts for all of the compounds are around 75 nm in the mesophase, *i.e.* higher than those obtained in solution (by *ca.* 40 nm). This indicates lower energy of the emissive aggregates in the liquid crystalline medium compared to the monomer species in THF diluted solution, likely related to significant structural relaxation processes of the excited state in the former.[30b,32]

Variations of the emission maximum wavelength among the different compounds in the mesophase seem to be related to their different mesomorphic arrangements. The emission maxima of both nematic mesogens appear around 404 nm. As far as columnar mesomorphic materials are concerned, it can be observed that their corresponding emission maximum wavelengths are slightly higher than those of calamitic compounds: *i.e.* $\mathbf{C_3B9}$ (407 nm), $\mathbf{C_{10}B6}$ (412 nm) and $\mathbf{C_3B6}$ (413 nm). The model proposed for $\mathbf{C_3B9}$, in which π-conjugated cores are randomly distributed between columns, could be a tentative justification of the shorter emission λ_{max} observed for this compound with respect to mesogens derived from acid **B6**. For $\mathbf{C_3B6}$ and $\mathbf{C_{10}B6}$, the whole molecule is included within the same column, and this situation could limit conformational freedom and favour interactions between fluorophores[14a] larger than in $\mathbf{C_3B9}$. Nevertheless, the most significant red shift within this series was observed for compound $\mathbf{C_3B6^*}$, which shows an emission maximum at 422 nm. The optical activity found in the mesophase of $\mathbf{C_3B6^*}$ is consistent with a helical arrangement of the mesogens, which could likely be responsible for a higher level of organization of the π-conjugated cores and hence for its largest red-shifted emission.[33]

Electroactive properties

In view of the potential applications in optoelectronics of molecules like those described above, it is important to consider the relative facility to inject holes and electrons, respectively, into the material. This can be approximated from the molecular electrochemical properties, which were investigated for $\mathbf{C_3B6}$ and $\mathbf{C_3B9}$ by cyclic voltammetry (CV) in oxygen-free THF solutions. The voltammograms registered for $\mathbf{C_3B6}$ and $\mathbf{C_3B9}$ are presented in Fig. 6. Only one irreversible process can be observed in the oxidation region and a reduction process appears at negative potentials for both compounds. This reduction process was not visible when the scan was carried out following the sequence 0 V → −2 V → 2 V → 0 V (see ESI†). Likely, the oxidized species of such bulky molecules, with many aliphatic tails surrounding the conjugated core, evolves and this makes the redox processes difficult. This may be also the reason for the poor-resolved recorded voltammograms.

The HOMO and LUMO energy levels referred to the vacuum level have been estimated by combining electrochemical and optical data, and values are summarized in Table 6. The HOMO was determined from the oxidation potential by the empirical relationship: HOMO = $-(E^{ox}_{onset} + 4.4)$ eV where E^{ox}_{onset} is the onset potential for the oxidation wave relative to the Ag/AgCl reference electrode.[34] HOMO values for $\mathbf{C_3B6}$ and $\mathbf{C_3B9}$ were estimated as −5.7 and −5.8 eV, respectively. The LUMO was deduced from the optical band gap using the expression: LUMO = HOMO + ΔE_g, and was found to be −2.4 and −2.5 eV for $\mathbf{C_3B6}$ and $\mathbf{C_3B9}$, respectively.

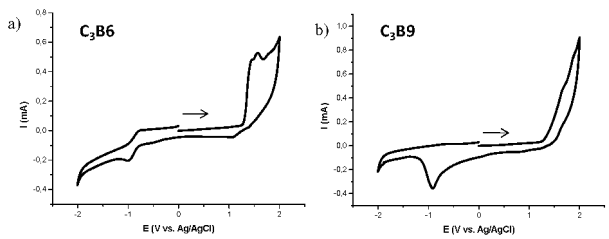

Fig. 6 Voltammograms corresponding to (a) $\mathbf{C_3B6}$ and (b) $\mathbf{C_3B9}$ recorded at a scan rate of 100 mV s^{-1}.

Table 6 Oxidation and reduction potentials estimated for the HOMO and LUMO levels of $\mathbf{C_3B6}$ and $\mathbf{C_3B9}$ in THF solutions

Compound	E^{ox}_{onset}/V	λ_{onset}[a]/nm	ΔE_g[b]/eV	HOMO[c]/eV	LUMO[d]/eV
$\mathbf{C_3B6}$	1.31	374	3.3	−5.7	−2.4
$\mathbf{C_3B9}$	1.39	375	3.3	−5.8	−2.5

[a] λ_{onset} was determined as the wavelength at which the absorbance is 0.05. [b] ΔE_g is the optical bandgap determined from the absorption spectra. [c] HOMO energy was determined by cyclic voltammetry according to the equation HOMO = $-(E^{ox}_{onset} + 4.4)$ eV, assuming the energy level of Ag/AgCl to be 4.4 eV below the vacuum level; [d] LUMO energy was calculated as HOMO + ΔE_g.

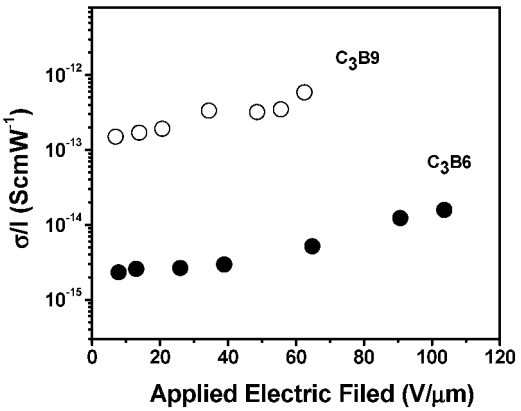

Fig. 7 Photoconductivity of **C_3B6** (homeotropically aligned, 4.0 μm thick sample; α = 80 cm^{-1}) and **C_3B9** (partially aligned, 7.5 μm thick sample; α = 75 cm^{-1}) as a function of the applied electric field, at λ = 532 nm.

Room temperature photoconductivity measurements for compounds **C_3B6** and **C_3B9** were performed as a function of wavelength and electric field on samples that were aligned as homeotropic monodomains or, at least, partially aligned. Photoconductivity shows the usual electric field dependence (Fig. 7). As expected, the photoconductivity of both **C_3B6** and **C_3B9** increases with absorption but even at λ = 532 nm, where absorption is quite small, a photoconduction signal can be measured. It is not as easy as it may seem to benchmark such values of photoconductivity against those of other columnar mesophases. In fact, often only charge mobilities are reported in the literature, even when transporters are photogenerated. In addition, experimental results are reported only in terms of photocurrents (often in arbitrary units) instead of photoconductivity and the absorption coefficient at the wavelength used is seldom indicated. All this hinders a comparison among different substances. However, it is possible to compare our results with the photoconductivity of other organic substances. Our materials show a photoconductivity which is of the same order of magnitude as the photoconductivity of the amorphous polymers[35] often used as photoconductors, but much lower than in crystalline composite organic solids.[36]

Experimental section

Synthesis

Synthesis of the core C_{10}

Synthesis of (E)*-1,6-bis[4-(*tert*-butyldimethylsilyloxy)phenyl]-3,4-didecyl-3-hexen-1,5-diyne (***2***).* To a solution of decylacetylene (631.9 mg, 0.812 mL, 3.8 mmol) in THF (50 mL) at −78 °C was added dropwise 2.26 mL of *n*-BuLi (1.6 M, 3.6 mmol). After 5 min, the carbene complex **1** (1.1 g, 2.0 mmol) was added and the resulting mixture was stirred at −78 °C until disappearance of the carbene complex (the solution turned from red to light yellow). Then, TMSOTf (0.68 mL, 3.8 mmol) was added to one portion and the mixture was stirred at −78 °C for 5 min. Finally, 56 mg (0.5 mmol) of potassium *tert*-butoxide (KO*t*Bu) were added and the mixture was transferred to a cold bath at −20° allowing it to warm up until colour change was observed. Removal of the solvents under reduced pressure followed by column chromatography of the residue on silica gel (hexane, R_f = 0.25) yielded **3** as a yellow solid (764 mg, 96%). ^{1}H NMR (400 MHz, $CDCl_3$, 25 °C, TMS): δ (ppm) = 7.37 (d, J = 8.7 Hz, 4H), 6.84 (d, J = 8.7 Hz, 4H), 2.64–2.53 (m, 4H), 1.77–1.58 (m, 4H), 1.48–1.25 (m, 28H), 1.03 (s, 18H), 0.98–0.87 (m, 6H), 0.25 (s, 12 H). ^{13}C NMR ($CDCl_3$, 100 MHz, 25 °C): δ (ppm) = 155.8 (C), 132.7 (CH), 129.0 (C), 120.1 (CH), 116.6 (C), 98.2 (C), 88.3 (C), 34.9 (CH_2), 31.9 (CH_2), 29.6 (CH_2), 29.5 (CH_2), 29.3 (CH_2), 29.0 (CH_2), 28.5 (CH_2), 25.6 (CH_3), 22.7 (CH_2), 18.2 (C), 14.1 (CH_3), −4.5 (CH_3). HRMS (EI) for $C_{36}H_{52}O_2Si_2$ $[M]^+$: 768.5691; found: 768.5698.

Synthesis of (E)*-1,6-bis(4-hydroxyphenyl)-3,4-didecyl-3-hexen-1,5-diyne (***C_{10}***).* To a solution of **2** (538.5 mg, 0.7 mmol) in THF (30 mL)/DMF (10 mL) at 25 °C was added 2 mL of saturated KF water solution. After 1 hour, 20 mL of water was added and the product was extracted with diethylether (3 × 20 mL). The organic layer was dried over anhydrous sodium sulfate and concentrated *in vacuo*. The crude product was triturated with hexane to yield **C_{10}** as a yellow solid (337 mg, 89%). Mp = 70–72 °C. ^{1}H NMR (400 MHz, $CDCl_3$, 25 °C, TMS): δ (ppm) = 7.39 (d, J = 8.0 Hz, 4H), 6.85 (d, J = 8.4 Hz, 4H), 5.75 (br s, 2H), 2.62 (t, J = 7.2 Hz, 4H), 1.72–1.69 (m, 4H), 1.58–1.18 (m, 28H), 1.01–0.82 (m, 6H). ^{13}C NMR ($CDCl_3$, 100 MHz, 25 °C): δ (ppm) = 155.3 (C), 132.9 (CH), 129.0 (C), 116.1 (C), 115.5 (CH), 98.1 (C), 88.2 (C), 34.9 (CH_2), 31.8 (CH_2), 29.6 (CH_2), 29.4 (CH_2), 29.3 (CH_2), 29.0 (CH_2), 28.4 (CH_2), 22.6 (CH_2), 14.0 (CH_3). HRMS (EI) for $C_{24}H_{24}O_2$ $[M]^+$: 540.3962; found: 540.3973.

Synthesis and characterization of the chiral acid, B6*. The benzoic acid **B6*** was synthesized according to the general procedure described for the synthesis of acid **B6**.[18b] (*S*)-3,7-Dimethyloctyl bromide was prepared from (*S*)-8-bromo-2,6-dimethyloct-2-ene by hydrogenation at high pressure using PtO_2 as catalyst.[37]

*Ethyl 3,4-bis[(*S*)-3,7-dimethyloctyloxy]benzoate.* This product was purified by flash chromatography on silica gel, eluting with a mixture hexane/dichloromethane (60/40). A colourless oil was obtained with a yield of 90%. R_f: 0.45 (hexane/dichloromethane, 60/40). ^{1}H-NMR (400 MHz, $CDCl_3$): δ (ppm) = 0.8–0.88 (m, 12H, $(CH_3)_2CH$), 0.94–0.96 (m, 6H, $CH(CH_3)CH_2$), 1.12–1.40 (m, 15H, $CH(CH_3)CH_2CH_2CH_2CH$ + $COOCH_2CH_3$), 1.58–1.74 (m, 6H, CH_2CH_2OAr + $CH(CH_3)CH_2$ + $(CH_3)_2CH$), 1.84–1.92 (m, 2H, CH_2CH_2OAr), 4.00–4.11 (m, 4H, CH_2CH_2OAr), 4.35 (*c*, 2H, J = 7.1 Hz, $COOCH_2CH_3$), 6.86 (d, 1H, J = 6.4 Hz, Ar-*H*), 7.54 (d, 1H, J = 2.0 Hz Ar-*H*), 7.64 (dd, 1H, J = 6.4 Hz, J = 2.0 Hz, Ar-*H*). ^{13}C-NMR (400 MHz, $CDCl_3$): δ (ppm) = 14.4, 19.7, 22.6, 22.7, 24.7, 28.0, 29.9, 36.0, 36.1, 37.3, 39.2, 60.7, 67.4, 67.6, 111.7, 114.0, 122.7, 123.4, 148.4, 153.0, 166.5. IR (nujol, NaCl): 1715, 1600, 1514, 1286, 1270, 1212, 1132, 1105 cm^{-1}.

*3,4-Bis[(*S*)-3,7-dimethyloctyloxy]benzyl alcohol.* The colourless oil obtained upon reduction of the ethylester group was used in the next reaction step without further purification. R_f: 0.76 (hexane/ethyl acetate, 70/30). ^{1}H-NMR (400 MHz, $CDCl_3$): δ (ppm) = 0.85–0.88 (m, 12H, $(CH_3)_2CH$), 0.93–0.95 (m, 6H, $CH(CH_3)CH_2$), 1.12–1.38 (m, 12H, $CH(CH_3)CH_2CH_2CH_2CH$), 1.47–1.71 (m, 6H, CH_2CH_2OAr + $CH(CH_3)CH_2$ + $(CH_3)_2CH$), 1.82–1.91 (m, 2H, CH_2CH_2OAr), 3.98–4.06 (m, 4H, CH_2CH_2OAr),

4.61 (s, 2H, ArCH_2OH), 6.85–6.86 (m, 2H, Ar-*H*), 6.93 (s, 1H, Ar-*H*). ^{13}C-NMR (400 MHz, $CDCl_3$): δ (ppm) = 19.7, 22.6, 22.7, 24.7, 28.0, 29.9, 36.2, 36.3, 37.3, 39.2, 65.4, 67.5, 67.7, 112.8, 113.7, 119.5, 133.6, 148.7, 149.3. IR (nujol, NaCl): 3600–3300, 1606, 1590, 1513, 1263, 1235, 1163, 1137 cm^{-1}.

3,4-Bis[(*S*)-3,7-dimethyloctyloxy]benzyl chloride. The product was used immediately in the next reaction step without further purification.

^{1}H-NMR (400 MHz, $CDCl_3$): δ (ppm) = 0.85–0.88 (m, 12H, (CH_3)$_2$CH), 0.93–0.95 (m, 6H, CH(CH_3)CH$_2$), 1.10–1.38 (m, 12H, CH(CH$_3$)CH_2CH_2CH_2CH), 1.47–1.72 (m, 6H, CH_2CH$_2$OAr + CH(CH$_3$)CH$_2$ + (CH$_3$)$_2$CH), 1.82–1.91 (m, 2H, CH_2CH$_2$OAr), 3.98–4.06 (m, 4H, CH$_2$CH_2OAr), 4.55 (s, 2H, ArCH_2Cl), 6.26 (d, 1H, J = 8.0 Hz, Ar-*H*), 6.88–6.92 (m, 2H, Ar-*H*). ^{13}C-NMR (400 MHz, $CDCl_3$): δ (ppm) = 19.7, 22.6, 22.7, 24.7, 28.0, 29.9, 36.2, 37.3, 39.3, 65.4, 67.5, 67.7, 112.9, 113.7, 119.5, 133.6, 148.7, 149.4. IR (nujol, NaCl): 1606, 1590, 1515, 1264, 1236, 1169, 1136 cm^{-1}.

*Methyl 3,4,5-tris[3′,4′-bis((*S*)-3,7-dimethyloctyloxy)benzyloxy]-benzoate*. This product was purified by flash chromatography on silica gel, eluting with a mixture dichloromethane/hexane (80/20). A colourless oil was obtained with a 37% yield. R_f: 0.66 (hexane/ethyl acetate, 85/15). ^{1}H-NMR (400 MHz, $CDCl_3$) δ (ppm) = 0.84–0.95 (m, 54H, CH_3), 1.08–1.38 (m, 36H, CH(CH$_3$)CH_2CH_2CH_2CH), 1.44–1.74 (m, 18H, CH_2CH$_2$OAr + CH$_2$CH(CH$_3$) + (CH$_3$)$_2$CH), 1.79–1.91 (m, 6H, CH_2CH$_2$OAr), 3.78–3.84 (m, 2H, CH$_2$CH_2OAr), 3.87 (s, 3H, COOCH_3), 3.92–4.04 (m, 10H, CH$_2$CH_2OAr), 5.03–5.04 (m, 6H, ArCH_2OAr), 6.72 (d, 1H, J = 8.2 Hz, Ar-H), 6.83–6.86 (m, 3H, Ar-*H*), 6.93 (dd, 2H, J = 8.2 Hz, J = 1.8 Hz, Ar-*H*), 6.96 (d, 1H, J = 1.8 Hz, Ar-*H*), 6.99 (d, 2H, J = 1.8 Hz), 7.36 (s, 2 H, Ar-*H*). ^{13}C-NMR (400 MHz, $CDCl_3$) δ (ppm) = 19.5–19.7, 22.6–22.7, 24.7, 28.0, 29.7–30.0, 36.3, 37.4, 39.3, 52.2, 67.2, 67.5–67.6, 71.4, 74.9, 109.9, 113.2, 113.3, 113.5, 114.0, 120.2, 121.1, 125.0, 129.2, 130.0, 142.5, 148.9–149.0, 149.2, 152.6, 166.6. IR (nujol, NaCl): 1718, 1590, 1516, 1265, 1230, 1169, 1138 cm^{-1}. MS (MALDI$^+$, dithranol) m/z: 1414 [M + Na]$^+$. Elemental analysis calculated for $C_{89}H_{146}O_{11}$ (1392.10): C, 76.79%; H, 10.57%; found: C, 76.94%; H, 10.42%.

*3,4,5-Tris[3′,4′-bis((*S*)-3,7-dimethyloctyloxy)benzyloxy]benzoic acid,* **B6***. **B6*** was purified by flash chromatography on silica gel, eluting with a mixture dichloromethane/hexane/ethyl acetate (40/60/2). A transparent wax was obtained with a yield of 50%. R_f: 0.15 (hexane/ethyl acetate, 80/20). ^{1}H-NMR (400 MHz, $CDCl_3$): δ (ppm) = 0.84–0.95 (m, 54H, CH_3), 1.08–1.38 (m, 36H, CH(CH$_3$)CH_2CH_2CH_2CH), 1.44–1.74 (m, 18H, CH_2CH$_2$OAr + CH(CH$_3$)CH$_2$ + (CH$_3$)$_2$CH), 1.79–1.91 (m, 6H, CH_2CH$_2$OAr), 3.78–3.85 (m, 2H, CH$_2$CH_2OAr), 3.94–4.05 (m, 10H, CH$_2$CH_2OAr), 5.06 (s, 6H, ArCH_2OAr), 6.73 (d, 1H, J = 8.2 Hz, Ar-*H*), 6.84–6.87 (m, 3H, Ar-*H*), 6.94 (dd, 2H, J = 8.2, J = 1.8 Hz, Ar-*H*), 6.97 (d, 1H, J = 1.8 Hz, Ar-*H*), 7.00 (d, 2H, J = 1.8 Hz, Ar-*H*), 7.43 (s, 2H, Ar-*H*). ^{13}C-NMR (400 MHz, $CDCl_3$): δ (ppm) = 19.5–19.7, 22.6–22.7, 24.7, 28.0, 29.8–29.9, 36.3, 37.4, 39.2, 67.2, 67.5–67.6, 71.4, 74.9, 109.9, 113.1, 113.2, 113.4, 113.9, 120.2, 121.1, 123.8, 129.1, 129.9, 143.1, 148.9–149.0, 149.2, 152.6, 170.1. IR (nujol, NaCl): 1716, 1689, 1590, 1516, 1265, 1230, 1169, 1138 cm^{-1}. MS (MALDI$^+$, dithranol) m/z: 1400 [M + Na]$^+$. Elemental analysis: calculated for $C_{88}H_{144}O_{11}$ (1378.08): C, 76.70%; H, 10.53%; found: C, 76.88%; H, 10.48%.

Synthesis and chemical information of final compounds CA and CB. Coupling of acid derivatives **A** and **B** with either $\mathbf{C_3}$ or $\mathbf{C_{10}}$ to give the target compounds was carried out by following the same procedure as described previously for $\mathbf{C_3B9}$.[15] The protons noted as H′ correspond to protons of the lateral chain of the central cores $\mathbf{C_3}$ and $\mathbf{C_{10}}$, so that they are distinguished from protons corresponding to the acid moiety.

*(*E*)-1,6-Bis[4′-(4″-*n*-dodecyloxybenzoyloxy)phenyl]-3,4-dipropyl-3-hexen-1,5-diyne,* $\mathbf{C_3A1}$. $\mathbf{C_3A1}$ was purified by chromatography on silica gel, eluting with a dichloromethane/hexane (50/50) mixture, and a white solid was obtained (73%). R_f: 0.51 (dichloromethane/hexane, 60/40). ^{1}H-NMR (400 MHz, $CDCl_3$): δ (ppm) = 0.89 (t, 6H, J = 6.8 Hz, CH_3), 1.02 (t, 6H, J = 7.4 Hz, CH_3′), 1.25–1.40 (m, 32H, (CH_2)$_8$), 1.44–1.51 (m, 4H, OCH$_2$CH$_2$CH_2), 1.66–1.75 (m, 4H, CH_2′CH$_3$′), 1.79–1.86 (m, 4H, OCH$_2$CH_2), 2.58 (t, 4H, J = 7.4 Hz, C≡CCH_2′), 4.05 (t, 4H, J = 6.6 Hz, OCH_2), 6.97 (d, 4H, J = 8.9 Hz, Ar-*H*), 7.19 (d, 4H, J = 8.7 Hz, Ar-*H*), 7.50 (d, 4H, J = 8.7 Hz, Ar-*H*), 8.13 (d, 4H, J = 8.9 Hz, Ar-*H*). ^{13}C-NMR (400 MHz, $CDCl_3$): δ (ppm) = 13.7, 14.1, 21.9, 22.7, 26.0, 29.1–29.7, 31.9, 37.1, 68.3, 89.3, 97.8, 114.3, 121.1, 121.2, 121.9, 129.6, 132.3, 132.5, 150.8, 163.6, 164.5. IR (KBr): 1730, 1606, 1510, 1504, 1467, 1254, 1203, 1163, 1067 cm^{-1}. MS (MALDI$^+$, dithranol) m/z: 922 [M + H]$^+$. Elemental analysis calculated for $C_{62}H_{80}O_6$ (921.30): C, 80.83%; H, 8.75%; found: C, 80.41%; H, 8.83%.

*(*E*)-1,6-Bis[4′-(4″-*n*-dodecyloxybenzoyloxy)phenyl]-3,4-didecyl-3-hexen-1,5-diyne,* $\mathbf{C_{10}A1}$. $\mathbf{C_{10}A1}$ was purified by chromatography on silica gel, eluting with a dichloromethane/hexane (40/60) mixture, and a white solid was obtained (65%). R_f: 0.78 (dichloromethane/hexane, 60/40). ^{1}H-NMR (400 MHz, $CDCl_3$): δ (ppm) = 0.85–0.90 (m, 12H, CH_3 + CH_3′), 1.20–1.51 (m, 64H, (CH_2)$_9$ + (CH_2′)$_7$), 1.63–1.70 (m, 4H, C≡CH$_2$′CH_2′), 1.79–1.86 (m, 4H, OCH$_2$CH_2), 2.58 (t, 4H, J = 7.4 Hz, C≡CCH_2′), 4.05 (t, 4H, J = 6.6 Hz, OCH_2), 6.97 (d, 4H, J = 8.9 Hz, Ar-*H*), 7.19 (d, 4H, J = 8.7 Hz, Ar-*H*), 7.50 (d, 4H, J = 8.7 Hz, Ar-*H*), 8.13 (d, 4H, J = 8.9 Hz, Ar-*H*). ^{13}C-NMR (400 MHz, $CDCl_3$): δ (ppm) = 14.1, 22.7, 26.0, 28.5, 29.1–29.7, 31.9, 35.0, 68.3, 89.3, 97.8, 114.3, 121.1, 121.2, 121.9, 129.7, 132.3, 132.5, 150.8, 163.6, 164.6. IR (KBr): 1742, 1606, 1509, 1502, 1466, 1257, 1206, 1162, 1074 cm^{-1}. MS (MALDI$^+$, dithranol) m/z: 1118 [M + H]$^+$. Elemental analysis calculated for $C_{76}H_{108}O_6$ (1117.67): C, 81.67%; H, 9.74%; found: C, 81.43%; H, 9.59%.

*(*E*)-1,6-Bis[4′-(3″,4″-*di*-n-dodecyloxybenzoyloxy)phenyl]-3,4-dipropyl-3-hexen-1,5-diyne,* $\mathbf{C_3A2}$. $\mathbf{C_3A2}$ was purified by chromatography on silica gel, eluting with a dichloromethane/hexane (50/50) mixture, and a white solid was obtained (68%). R_f: 0.69 (dichloromethane/hexane, 60/40). ^{1}H-NMR (400 MHz, $CDCl_3$): δ (ppm) = 0.86–0.90 (t, 12H, CH_3), 1.02 (t, 6H, J = 7.4 Hz, CH_3′), 1.22–1.42 (m, 64H, (CH_2)$_8$), 1.44–1.53 (m, 8H, OCH$_2$CH$_2$CH_2), 1.67–1.76 (m, 4H, CH_2′CH$_3$′), 1.81–1.90 (m, 8H, OCH$_2$CH_2), 2.58 (t, 4H, J = 7.4 Hz, C≡CCH_2′), 4.05–4.10 (m, 8H, OCH_2),

6.93 (d, 2H, J = 8.5 Hz, Ar-*H*), 7.19 (d, 4H, J = 8.7 Hz, Ar-*H*), 7.50 (d, 4H, J = 8.7 Hz, Ar-*H*), 7.65 (d, 2H, J = 2.0 Hz, Ar-*H*), 7.81 (dd, 2H, ^3J = 8.5 Hz, ^4J = 2.0 Hz, Ar-*H*). ^{13}C-NMR (400 MHz, $CDCl_3$): δ (ppm) = 13.7, 14.1, 21.9, 22.7, 26.0, 29.1–29.7, 31.9, 37.1, 69.1, 69.4, 89.3, 97.8, 112.0, 114.6, 121.2, 121.3, 122.0, 124.4, 129.6, 132.5, 148.7, 150.9, 153.9, 164.8. IR (KBr): 1730, 1597, 1519, 1505, 1467 , 1294, 1273, 1254, 1198, 1163, 1143 cm^{-1}. MS (MALDI$^+$, dithranol) m/z: 1312 [M + Na]$^+$. Elemental analysis calculated for $C_{86}H_{128}O_8$ (1289.93): C, 80.08%; H, 10.00%; found: C, 79.71%; H, 9.96%.

*(*E*)-1,6-Bis[4′-(3″,4″-di-*n*-dodecyloxybenzoyloxy)phenyl]-3,4-didecyl-3-hexen-1,5-diyne,* **C_{10}A2**. **C_{10}A2** was purified by chromatography on silica gel, eluting with a dichloromethane/hexane (40/60) mixture, and a white solid was obtained (71%). R_f: 0.57 (dichloromethane/hexane, 50/50). ^{1}H-NMR (400 MHz, $CDCl_3$): δ (ppm) = 0.85–0.90 (t, 18H, CH_3 + CH_3'), 1.22–1.52 (m, 100H, $(CH_2)_9$ + $(CH_2')_7$), 1.63–1.70 (m, 4H, $CH_2'CH_3'$), 1.81–1.90 (m, 8H, OCH_2CH_2), 2.58 (t, 4H, J = 7.4 Hz, C≡CCH_2'), 4.05–4.10 (m, 8H, OCH_2), 6.93 (d, 2H, J = 8.5 Hz, Ar-*H*), 7.19 (d, 4H, J = 8.7 Hz, Ar-*H*), 7.50 (d, 4H, J = 8.7 Hz, Ar-*H*), 7.65 (d, 2H, J = 2.0 Hz, Ar-*H*), 7.82 (dd, 2H, ^3J = 8.5 Hz, ^4J = 2.0 Hz, Ar-*H*). ^{13}C-NMR (400 MHz, $CDCl_3$): δ (ppm) = 14.1, 22.7, 26.0, 28.5, 29.0–29.7, 31.9, 35.0, 69.1, 69.4, 89.3, 97.8, 111.9, 114.6, 121.2, 121.3, 121.9, 124.4, 129.7, 132.5, 148.7, 150.9, 153.9, 164.8. IR (KBr): 1729, 1598, 1517, 1505, 1467, 1292, 1274, 1252, 1200, 1164, 1143 cm^{-1}. MS (MALDI$^+$, dithranol) m/z: 1508 [M + Na]$^+$. Elemental analysis calculated for $C_{100}H_{156}O_8$ (1486.30): C, 80.81%; H, 10.58%; found: C, 80.79%; H, 10.63%.

*(*E*)-1,6-Bis[4′-(3″,4″,5″-tri-*n*-dodecyloxybenzoyloxy)phenyl]-3,4-dipropyl-3-hexen-1,5-diyne,* **C_3A3**. **C_3A3** was purified by chromatography on silica gel, eluting with a dichloromethane/hexane (50/50) mixture, and a white solid was obtained (64%). R_f: 0.59 (dichloromethane/hexane, 60/40). ^{1}H-NMR (400 MHz, $CDCl_3$): δ (ppm) = 0.88 (t, 18H, J = 6.6, CH_3), 1.02 (t, 6H, J = 7.4, CH_3'), 1.25–1.52 (m, H, $(CH_2)_9$), 1.67–1.88 (m, 16H, OCH_2CH_2 + C≡$CH_2'CH_2'$), 2.59 (t, 4H, J = 7.4 Hz, C≡CCH_2'), 4.01–4.08 (m, 12H, OCH_2), 7.18 (d, 4H, J = 8.7 Hz, Ar-*H*), 7.40 (s, 4H, Ar-*H*), 7.51 (d, 4H, J = 8.7 Hz, Ar-*H*). ^{13}C-NMR (400 MHz, $CDCl_3$): δ (ppm) = 13.7, 14.1, 21.9, 22.7, 26.1, 29.3–29.7, 30.3, 31.9, 37.1, 69.2, 73.6, 89.3, 97.8, 108.5, 121.3, 121.9, 123.6, 129.6, 132.5, 143.0,150.8, 152.9, 164.8. IR (KBr): 1738, 1588, 1505, 1467, 1230, 1195, 1162, 1133, 1125 cm^{-1}. MS (MALDI$^+$, dithranol) m/z: 1658 [M + H]$^+$. Elemental analysis calculated for $C_{110}H_{176}O_{10}$ (1658.57): C, 79.66%; H, 10.70%; found: C, 79.59%; H, 10.69%.

*(*E*)-1,6-Bis[4′-(3″,4″,5″-tri-*n*-dodecyloxybenzoyloxy)phenyl]-3,4-didecyl-3-hexen-1,5-diyne,* **C_{10}A3**. **C_{10}A3** was purified by chromatography on silica gel, eluting with a dichloromethane/hexane (40/60) mixture, and a white solid was obtained (59%). R_f: 0.60 (dichloromethane/hexane, 50/50). ^{1}H-NMR (400 MHz, $CDCl_3$): δ (ppm) = 0.85–0.90 (m, 24H, CH_3 + CH_3'), 1.23–1.52 (m, 136H, $(CH_2)_9$ + $(CH_2)_7$), 1.63–1.70 (m, 4H, C≡$CH_2'CH_2'$), 1.73–1.87 (m, 12H, OCH_2CH_2), 2.59 (t, 4H, J = 7.4 Hz, C≡CCH_2'), 4.03–4.08 (m, 12H, OCH_2), 7.17 (d, 4H, J = 8.7 Hz, Ar-*H*), 7.40 (s, 4H, Ar-*H*), 7.50 (d, 4H, J = 8.7 Hz, Ar-*H*). ^{13}C-NMR (400 MHz, $CDCl_3$): δ (ppm) = 14.1, 22.7, 26.0, 26.1, 28.5, 29.1–29.7, 30.3, 31.9, 32.0, 35.0, 69.2, 73.6, 89.4, 97.8, 108.5, 121.3, 121.9, 123.6, 129.70, 132.5, 143.1, 150.8, 153.0, 164.8. IR (KBr): 1735, 1587, 1505, 1468 , 1231, 1198, 1164, 1130, 1121 cm^{-1}. MS (MALDI$^+$, dithranol) m/z: 1855 [M + H]$^+$. Elemental analysis calculated for $C_{124}H_{204}O_{10}$ (1854.94): C, 80.29%; H, 11.08%; found: C, 80.12%; H, 10.79%.

*(*E*)-1,6-Bis{4′-[3″,4″,5″-tris(4‴-*n*-dodecyloxybenzyloxy)benzoyloxy]phenyl}-3,4-dipropyl-3-hexen-1,5-diyne,* **C_3B3**. **C_3B3** was purified by chromatography on silica gel, eluting with a dichloromethane/hexane/ether (70/30/1) mixture, and a white solid was obtained (55–60%). R_f: 0.40 (dichloromethane/hexane, 80/20). ^{1}H-NMR (400 MHz, $CDCl_3$): δ (ppm) = 0.88 (t, 18H, J = 6.8 Hz, CH_3), 1.03 (t, 6H, J = 7.4 Hz, CH_3'), 1.25–1.50 (m, 108H, $(CH_2)_9$), 1.69–1.83 (m, 16H, OCH_2CH_2 + $CH_2'CH_3'$), 2.59 (t, 4H, J = 7.4 Hz, C≡CCH_2'), 3.91–3.98 (m, 12H, OCH_2), 5.06 (s, 4H, OCH_2Ar), 5.08 (s, 8H, OCH_2Ar), 6.77 (d, 4H, J = 8.7 Hz, Ar-*H*), 6.90 (d, 8H, J = 8.7 Hz, Ar-*H*), 7.18 (d, 4H, J = 8.7 Hz, Ar-*H*), 7.27 (d, 4H, J = 8.6 Hz, Ar-*H*), 7.35 (d, 8H, J = 8.7 Hz, Ar-*H*), 7.50–7.52 (m, 8H, Ar-*H*). ^{13}C-NMR (400 MHz, $CDCl_3$): δ (ppm) = 13.7, 14.1, 21.9, 22.7, 26.1, 29.3–29.7, 31.9, 37.1, 68.0, 68.1, 71.2, 74.7, 89.4, 97.8, 109.8, 114.1, 114.5, 121.3, 121.9, 123.9, 128.4, 129.3, 129.7, 130.3, 132.5, 143.2, 150.7, 152.7, 159.0, 159.1, 164.5. IR (KBr): 1739, 1615, 1585, 1515, 1504, 1250, 1189, 1174, 1127 cm^{-1}. MS (MALDI$^+$, dithranol) m/z: 2317 [M + Na]$^+$. Elemental analysis calculated for $C_{152}H_{212}O_{16}$ (2295.30): C, 79.54%; H, 9.31%; found: C, 79.48%; H, 9.49%.

*(*E*)-1,6-Bis{4′-[3″,4″,5″-tris(4‴-*n*-dodecyloxybenzyloxy)benzoyloxy]phenyl}-3,4-didecyl-3-hexen-1,5-diyne,* **C_{10}B3**. **C_{10}B3** was purified by chromatography on silica gel, eluting with a dichloromethane/hexane/ether (60/40/1) mixture, then the solid was washed with acetone to yield **C_{10}B3** as a white solid (54%). R_f: 0.39 (dichloromethane/hexane, 70/30). ^{1}H-NMR (400 MHz, $CDCl_3$): δ (ppm) = 0.86–0.90 (m, 24H, CH_3 + CH_3'), 1.25–1.50 (m, 136H, $(CH_2)_9$ + $(CH_2')_7$), 1.64–1.72 (m, 4H, $CH_2'CH_3'$), 1.74–1.83 (m, 12H, OCH_2CH_2), 2.60 (t, 4H, J = 7.4 Hz, C≡CCH_2'), 3.91–3.98 (m, 12H, OCH_2), 5.06 (s, 4H, OCH_2Ar), 5.08 (s, 8H, OCH_2Ar), 6.77 (d, 4H, J = 8.6 Hz, Ar-*H*), 6.90 (d, 8H, J = 8.6 Hz, Ar-*H*), 7.18 (d, 4H, J = 8.6 Hz, Ar-*H*), 7.27 (d, 4H, J = 8.6 Hz, Ar-*H*), 7.35 (d, 8H, J = 8.6 Hz, Ar-*H*), 7.50–7.52 (m, 8H, Ar-*H*). ^{13}C-NMR (400 MHz, $CDCl_3$): δ (ppm) = 14.1, 22.7, 26.1, 28.5, 29.1–29.7, 31.9, 35.0, 68.0, 68.1, 71.2, 74.7, 89.4, 97.8, 109.8, 114.1, 114.5, 121.4, 121.9, 123.9, 128.4, 129.3, 129.7, 130.3, 132.5, 143.2, 150.7, 152.7, 159.0, 159.1, 164.5. IR (KBr): 1734, 1615, 1587, 1516, 1504, 1248, 1190, 1173, 1120 cm^{-1}. MS (MALDI$^+$, dithranol) m/z: 2513 [M + Na]$^+$. Elemental analysis calculated for $C_{166}H_{240}O_{16}$ (2491.67): C, 80.02%; H, 9.71%; found: C, 79.82%; H, 9.63%.

*(*E*)-1,6-Bis{4′-[3″,4″,5″-tris(3‴,4‴-di-*n*-dodecyloxybenzyloxy)benzoyloxy]phenyl}-3,4-dipropyl-3-hexen-1,5-diyne,* **C_3B6**. **C_3B6** was purified by flash chromatography on silica gel, eluting with a dichloromethane/hexane/ether (60/40/1) mixture. Then the solid was washed with acetone to yield the product as a white solid (37–41%). R_f: 0.41 (dichloromethane/hexane, 70/30). ^{1}H-NMR (400 MHz, $CDCl_3$): δ (ppm) = 0.86–0.89 (m, 36H, CH_3), 1.03 (t, 6H, J = 7.4 Hz, CH_3'), 1.21–1.50 (m, 216H, $CH_3(CH_2)_9$),

1.70–1.85 (m, 28H, CH_2CH_2OAr + C = $CCH_2'CH_2'$), 2.59 (t, 4H, J = 7.4 Hz, C=CCH_2'), 3.77 (t, 4H, J = 6.5 Hz, CH_2OAr), 3.91–4.00 (m, 20H, CH_2OAr), 5.07–5.08 (m, 12H, $ArCH_2OAr$), 6.74 (d, 2H, J = 8.2 Hz, 6.84–6.86 (m, 6H, Ar-*H*), 6.94 (dd, 4H, ^3J = 8.2 Hz, ^5J = 1.8 Hz, Ar-*H*), 6.97 (d, 2H, J = 1.8 Hz, Ar-*H*), 7.00 (d, 2H, J = 1.8 Hz, Ar-*H*), 7.17 (d, 4H, J = 8.7 Hz, Ar-*H*), 7.50–7.52 (m, 8H, Ar-*H*). ^{13}C-NMR (400 MHz, $CDCl_3$) = 13.7, 14.1, 21.9, 22.7, 26.1–29.8, 31.9, 37.1, 69.0, 69.2, 69.3, 71.5, 89.4, 97.8, 110.0, 113.3, 113.4, 113.6, 114.1, 120.3, 121.1, 121.4, 121.9, 124.0, 129.1, 129.7, 130.0, 132.5, 143.2, 149.0, 149.1, 149.3, 150.7, 152.8, 164.5. IR (KBr): 1736 , 1593, 1519, 1505, 1269, 1228, 1193, 1139, 1117 cm^{-1}. MS ($MALDI^+$, dithranol) m/z: 3422 $[M + Na]^+$. Elemental analysis calculated for $C_{224}H_{356}O_{22}$ (3401.21): C, 79.10%; H, 10.55%; found: C, 78.93%; H, 10.56%.

*(*E*)-1,6-Bis{4′-[3″,4″,5″-tris(3‴,4‴-di-*n*-dodecyloxybenzyloxy)-benzoyloxy]phenyl}-3,4-didecyl-3-hexen-1,5-diyne,* **C_{10}B6**. This compound was purified by chromatography on silica gel, eluting with a dichloromethane/hexane/ether (55/45/1) mixture, then the solid was washed with acetone to yield **C_{10}B6** as a white solid (40%). R_f: 0.55 (dichloromethane/hexane, 70/30). ^{1}H-NMR (400 MHz, $CDCl_3$): δ (ppm) = 0.86–0.89 (m, 42H, CH_3 + CH_3'), 1.25–1.50 (m, 244H, $CH_3(CH_2)_9$ + $CH_3'(CH_2')_7$), 1.64–1.85 (m, 28H, CH_2CH_2OAr + C = $CCH_2'CH_2'$), 2.59 (t, 4H, J = 7.4 Hz, C=CCH_2') 3.76 (t, 4H, J = 6.5 Hz, CH_2OAr), 3.91–4.00 (m, 20H, CH_2OAr), 5.06–5.07 (m, 12H, $ArCH_2OAr$), 6.73 (d, 2H, J = 8.2 Hz), 6.84–6.86 (m, 6H, Ar-*H*), 6.94 (dd, 4H, ^3J = 8.2 Hz, ^5J = 1.8 Hz, Ar-*H*), 6.97 (d, 2H, J = 1.8 Hz, Ar-*H*), 7.00 (d, 4H, J = 1.8 Hz, Ar-*H*), 7.17 (d, 4H, J = 8.7 Hz, Ar-*H*), 7.49–7.51 (m, 8H, Ar-*H*). ^{13}C-NMR (400 MHz, $CDCl_3$): δ (ppm) = 14.1, 22.7, 26.1–29.8, 31.9, 35.0, 69.0, 69.2, 69.3, 71.5, 75.0, 89.4, 97.8, 110.0, 113.3, 113.4, 113.6, 114.1, 120.3, 121.1, 121.4, 121.9, 124.0, 129.1, 129.7, 130.0, 132.5, 143.2, 149.0, 149.1, 149.3, 150.7, 152.8, 164.5. IR (KBr): 1736, 1593, 1521, 1505, 1269, 1228, 1193, 1138, 1116 cm^{-1}. MS ($MALDI^+$, dithranol) m/z: 3618 $[M + Na]^+$. Elemental analysis calculated for $C_{238}H_{384}O_{22}$ (3597.58): C, 79.46%; H, 10.76%; found: C, 79.41%; H, 10.79%.

*(*E*)-1,6-Bis{4′-[3″,4″,5″-tris(3‴,4‴-bis((*S*)-3,7-dimethyloctyloxy)benzyloxy)benzoyloxy]phenyl}-3,4-dipropyl-3-hexen-1,5-diyne,* **C_3B6***. **C_3B6*** was purified by chromatography on silica gel, eluting with a dichloromethane/hexane/ether (55/45/1) mixture, then the crude product obtained was dissolved in dichloromethane and purified by precipitation with methanol to yield **C_3B6*** as opaque wax (32–35%). R_f: 0.46 (dichloromethane/hexane, 70/30). ^{1}H-NMR (500 MHz, $CDCl_3$) δ (ppm) = 0.84–0.95 (m, 108H, CH_3), 1.03 (t, 6H, J = 7.3 Hz, CH_3'), 1.09–1.37 (m, 72H, $(CH_3)_2CHCH_2CH_2CH_2$), 1.46–1.74 (m, 40H, $(CH_3)_2CH$ + $CH_2(CH_3)CHCH_2CH_2O$ + $(CH_3)_2CHCH_2$ + C=$CCH_2'CH_2'$), 1.78–1.90 (m, 12H, $CHCH_2CH_2O$), 2.59 (t, 4H, J = 7.3 Hz, $C{\equiv}CCH_2'$), 3.80–3.88 (m, 4H, CH_2OAr), 3.94–4.06 (m, 20H, CH_2OAr), 5.08–5.09 (m, 12H, $ArCH_2OAr$), 6.75 (d, 2H, J = 8.2 Hz), 6.85–6.88 (m, 6H, Ar-*H*), 6.95 (dd, 4H, J = 8.2 Hz, J = 1.7 Hz, Ar-*H*), 6.98 (d, 2H, J = 1.7 Hz, Ar-*H*), 7.00 (d, 4H, J = 1.7 Hz, Ar-*H*), 7.17 (d, 4H, J = 8.6 Hz, Ar-*H*), 7.50–7.51 (m, 8H, Ar-*H*). ^{13}C-NMR (500 MHz, $CDCl_3$) δ (ppm) = 19.5–19.7, 21.9, 22.6, 22.7, 24.7, 28.0, 29.8–30.0, 36.3–36.4, 37.0, 37.4–37.5, 39.3, 67.2, 67.5, 67.6, 71.5, 75.0, 89.4, 97.8, 110.0, 113.2, 113.3, 113.5, 114.0, 120.3, 121.2, 121.4, 121.9, 124.0, 129.1, 129.7, 129.9, 132.5, 143.2, 149.0, 149.2, 150.7, 152.8, 164.5. IR (KBr): 1736, 1591, 1516, 1286, 1232, 1187, 1164, 1139 cm^{-1}. MS ($MALDI^+$, dithranol) m/z: 3086 $[M + Na]^+$. Elemental analysis calculated for $C_{200}H_{308}O_{22}$ (3064.57): C, 78.49%; H, 10.12%; found: C, 78.38%; H, 10.13%.

*(*E*)-1,6-Bis{4′-[3″,4″,5″-tris(3‴,4‴,5‴-tri-*n*-dodecyloxybenzyloxy)benzoyloxy]phenyl}-3,4-didecyl-3-hexen-1,5-diyne,* **C_{10}B9**. This compound was purified by chromatography on silica gel, eluting with a dichloromethane/hexane/ether (55/45/1) mixture, then the solid was washed with acetone to yield **C_{10}B9** as a white solid (37%). R_f: 0.52 (dichloromethane/hexane, 70/30). ^{1}H-NMR (400 MHz, $CDCl_3$): δ (ppm) = 0.86–0. 90 (m, 60H, CH_3 + CH_3'), 1.22–1.51 (m, 352H, $CH_3(CH_2)_9$ + $CH_3(CH_2')_7$), 1.64–1.77 (m, 40H, CH_2CH_2OAr + $CH_2'CH_2'C{\equiv}C$), 2.60 (t, 4H, J = 7.3 Hz, $CH_2'C{\equiv}C$) 3.78 (t, 8H, J = 6.3 Hz, CH_2CH_2OAr), 3.87–3.95 (m, 28H, CH_2CH_2OAr), 5.07–5.09 (m, 12H, $ArCH_2O$), 6.62 (s, 4H, Ar-*H*), 6.65 (s, 8H, Ar-*H*), 7.16 (d, 4H, J = 8.6 Hz, Ar-*H*), 7.49–7.52 (m, 8H, Ar-*H*). ^{13}C-NMR (500 MHz, $CDCl_3$) δ (ppm) = 14.1, 22.7, 26.2–30.4, 31.9, 35.0, 68.9, 69.1, 71.7, 73.3, 73.4, 75.2, 89.4, 97.7, 105.7, 106.2, 106.3, 110.1, 121.5, 121.8, 124.2, 129.7, 131.5, 132.2, 132.5, 137.8, 137.9, 143.2, 150.6, 152.7, 153.0, 153.3, 164.3. IR (KBr): 1739, 1592, 1506, 1234, 1192, 1164, 1119 cm^{-1}. MS ($MALDI^+$, dithranol) m/z: 4723 $[M + Na]^+$. Elemental analysis calculated for $C_{310}H_{528}O_{28}$ (4703.49): C, 79.16%; H, 11.31%; found: C, 79.11%; H, 11.01%.

Characterization techniques

^{1}H (300 and 400 MHz) and ^{13}C (100 MHz) were measured in $CDCl_3$ on a BRUKER ARX-300 and BRUKER AVANCE-400 instrument. IR spectra on NaCl pellets were recorded using a Thermo Nicolet Avatar 380 spectrophotometer. Mass spectra were obtained on a MICROFLEX Bruker ($MALDI^+$) spectrometer.

Differential scanning calorimetry (DSC) and thermogravimetric analysis (TGA) were performed with DSC-MDSC TA instruments Q-1000 and Q-2000; and TA Q-5000, respectively. Liquid crystal textures were studied using an Olympus BX-50 polarizing microscope equipped with a Linkam TMS91 hot stage and a CS196 hot-stage central processor. Microphotographs were taken with a digital camera Olympus DP12-2.

X-Ray diffraction measurements were carried out at room temperature using a Pinhole camera (Anton-Paar) operating with a point focused Ni-filtered Cu Kα beam. The scattering angle range of the X-ray set-up is between 2θ 1° and 40°. The sample was held in Lindemann glass capillaries (1 mm diameter) perfectly sealed and heated, when necessary, with a variable-temperature attachment. The diffraction patterns were collected on a flat photographic film perpendicular to the X-ray beam.

UV/Vis absorption spectra were collected on an ATI-Unicam UV4-200 instrument using 10^{-4} to 10^{-5} M solutions in THF. Mesophase measurements were carried out at room temperature in a cast film onto a quartz plate prepared by evaporation of the solvent (THF) and subsequent melting above the clearing point.

Fluorescence spectra were recorded with a Perkin-Elmer LS50B spectrophotometer within the wavelength range 340–700. Solution experiments were recorded in THF solutions of *ca.* 0.01 absorbance (concentrations 10^{-6} to 10^{-7} M) in 1 cm quartz cells. The relative quantum yields of fluorescence (Φ_F) were determined in THF solutions according to the equation:

$$\Phi_{unk} = \Phi_{std}(I_{unk}/A_{unk})(A_{std}/I_{std})(\eta_{std}/n_{unk})^2$$

where Φ_{std} is the fluorescence yield of DPA (diphenylanthracene) standard ($\Phi_{std} = 0.9$ in 1 M cyclohexane at 298 K), I_{unk} and I_{std} are the integrated areas of the emission peaks of the sample and the standard, respectively, A_{unk} and A_{std} are the absorbances of the sample and standard, respectively, at the excitation wavelength λ_{exc} (335 nm), and η_{unk} and η_{std} are the refractive indices of the solvents corresponding to the sample and standard solutions. In all cases, quantum yields have been determined as the average of three measurements.

Fluorescence measurements of the mesophase were recorded in thin films sandwiched between two quartz plates.

CD spectra were recorded on a Jasco J-810. Neat samples were prepared by casting a solution of the compound **C_3B6*** in dichloromethane onto a quartz plate.

The cyclic voltammetry experiments were performed on an Eco Chemie μAutolab electrochemical analyzer. All experiments were carried out in a three electrode compartment cell with a Pt wire counter electrode, a glassy carbon working electrode and an Ag/AgCl reference electrode. The supporting electrolyte used was 0.1 M tetrabutylammonium hexafluorophosphate solution in dry tetrahydrofuran and the cell containing the solution of the sample (0,24 mM) and the supporting electrolyte was purged with a nitrogen gas thoroughly before scanning for its oxidation and reduction properties. The HOMO values were calculated by using the following general equation: HOMO $= -E^{ox}{}_{onset} - 4.4$ eV; E_{red} cannot be directly obtained from the CV measurements because a stable anionic state was not experimentally accessible. Therefore, LUMO values were estimated from the relation LUMO $= \Delta E_g -$ HOMO, where ΔE_g was calculated according to the relationship $\Delta E_g = 1239.85/\lambda_{onset}$.

Cells for photoconductivity measurements were obtained by using ITO substrates with 1 mm wide, lithographically patterned, conducting electrodes. Cells were cleaned by sequential 30 min sonication in solutions of detergent, deionized (DI) water, acetone, and isopropanol and then dried at 80 °C for 2 hours in a vacuum oven. Two substrates were glued together, using either 1.8 μm or 5.0 μm spacers to control the thickness, which was later measured by interferometry. Cells were then filled by capillarity, by heating cells and materials above the melting temperature on a hot plate. In order to align the liquid crystal director, samples were annealed in a temperature controlled oven (INSTEC STC200).

Photoconductivity was obtained by applying a DC electric field and measuring the current through the sample, both in the dark and under illumination. Currents were measured by a Kethley 6517A electrometer, while illumination was provided either by a green diode laser ($I \approx 6.70$ W cm^{-2}) at $\lambda = 533$ nm or by a He–Ne laser ($I \approx 10$ W cm^{-2}) at 633 nm. As the current depends on light intensity I, photoconductivity data were then normalized with respect to I.

Conclusions

The self-organization characteristics of rod-like fluorophores **C_3** and **C_{10}** can be controlled by conjugation to different types of benzoic acid derivatives. This strategy allows functional materials to be obtained that combine mesomorphic architectures with luminescence and photoconducting properties.

Depending on the type of acid, the nature of the materials ranges from nematic liquid crystals, for compounds derived from 4-dodecyloxybenzoic acid, to columnar liquid crystals, for compounds that incorporate six or nine terminal tails, through crystalline solids, for compounds with either four or six terminal tails. Indeed, the size ratio between the rigid core and the carboxylate groups, which vary in bulk, is crucial to address self-organization, thus indicating the delicate balance of forces involved in liquid crystalline behaviour. As for the mesomorphic behaviour shown by these materials, it is worth noting the re-entrant feature of the Col_h mesophase in the heating process of compound **C_{10}B6** after a cold crystallization of the same mesophase. Also, the structure of the Col_h mesophase shown by compound **C_3B9** with half a molecule as the circular cross section of column is corroborated, *versus* the structure of the column in **C_3B6**, **C_{10}B6** and **C_3B6*** in which two columns form the stacking unit. Furthermore, the addition of stereogenic centers to terminal chains enables the transfer of molecular chirality to the columnar supramolecular organization in **C_3B6***.

As functional materials, all of the mesogenic compounds show luminescence in the mesophase and this indicates that the supramolecular architecture prevents quenching—in contrast to the situation in the crystal structure of the chromophores. These columnar materials behave as photoconductors, with values of the same order of magnitude as the photoconductivity of the amorphous polymers.

Acknowledgements

This work was supported by the MICINN projects MAT2009-14636-C03-01, CSD2006-00012, CTQ-2007-61048, FEDER founding (EU), Aragon Government, Principado Asturias (Project IB08-088) and the MiUR project PRIN 2007 (2007WJMF2W). The authors thank Dr J. Barberá for his kind help and useful discussions.

References

1 (*a*) C. Li, M. Liu, N. G. Pschirer, M. Baumgarten and K. Müllen, *Chem. Rev.*, 2010, **110**, 6817–6855; (*b*) H. Sasabe and J. Kido, *Chem. Mater.*, 2010, **23**, 621–630; (*c*) A. Pron, P. Gawrys, M. Zagorska, D. Djurado and R. Demadrille, *Chem. Soc. Rev.*, 2010, **39**, 2577–2632; (*d*) H. Dong, C. Wang and W. Hu, *Chem. Commun.*, 2010, **46**, 5211–5222; (*e*) A. C. Grimsdale, K. Leok Chan, R. E. Martin, P. G. Jokisz and A. B. Holmes, *Chem. Rev.*, 2009, **109**, 897–1091.
2 J. W. Steed and J. L. Atwood, *Supramolecular Chemistry*, Wiley, 2009.
3 J. A. A. W. Elemans, R. van Hameren, R. J. M. Nolte and A. E. Rowan, *Adv. Mater.*, 2006, **18**, 1251–1266.
4 M. R. Wasielewski, *Acc. Chem. Res.*, 2009, **42**, 1910–1921.
5 M. O'Neill and S. M. Kelly, *Adv. Mater.*, 2011, **23**, 566–584.
6 P. Samorí and F. Cacialli, *Functional Supramolecular Architectures for Organic Electronics and Nanotechnology*, Wiley-VCH, Weinheim, 2011.

7 (*a*) T. Kato, N. Mizoshita and K. Kishimoto, *Angew. Chem., Int. Ed.*, 2006, **45**, 38–68; (*b*) T. Kato, T. Yasuda, Y. Kamikawa and M. Yoshio, *Chem. Commun.*, 2009, 729–739.

8 M. Lehmann, *Chem.–Eur. J.*, 2009, **15**, 3638–3651.

9 W. Pisula, M. Zorn, J. Y. Chang, K. Müllen and R. Zentel, *Macromol. Rapid Commun.*, 2009, **30**, 1179–1202.

10 (*a*) B. R. Kaafarani, *Chem. Mater.*, 2011, **23**, 378–396; (*b*) S. Sergeyev, W. Pisula and Y. H. Geerts, *Chem. Soc. Rev.*, 2007, **36**, 1902–1929; (*c*) S. Laschat, A. Baro, N. Steinke, F. Giesselmann, C. Hägele, G. Scalia, R. Judele, E. Kapatsina, S. Sauer, A. Schreivogel and M. Tosoni, *Angew. Chem., Int. Ed.*, 2007, **46**, 4832–4887; (*d*) R. J. Bushby and O. R. Lozman, *Curr. Opin. Solid State Mater. Sci.*, 2002, **6**, 569–578.

11 (*a*) E. M. García-Frutos, U. K. Pandey, R. Termine, A. Omenat, J. Barberá, J. L. Serrano, A. Golemme and B. Gómez-Lor, *Angew. Chem., Int. Ed.*, 2011, **50**, 7399–7402; (*b*) T. Yasuda, T. Shimizu, F. Liu, G. Ungar and T. Kato, *J. Am. Chem. Soc.*, 2011, **133**, 13437–13444; (*c*) W. Pisula, X. Feng and K. Müllen, *Adv. Mater.*, 2010, **22**, 3634–3649; (*d*) K. Isoda, T. Yasuda and T. Kato, *Chem.–Asian J.*, 2009, **4**, 1619–1625; (*e*) M. Talarico, R. Termine, E. M. Garcia-Frutos, A. Omenat, J. L. Serrano, B. Gomez-Lor and A. Golemme, *Chem. Mater.*, 2008, **20**, 6589–6591; (*f*) Z. Chen, V. Stepanenko, V. Dehm, P. Prins, L. D. A. Siebbeles, J. Seibt, P. Marquetand, V. Engel and F. Würthner, *Chem.–Eur. J.*, 2007, **13**, 436–449; (*g*) A. Hayer, V. de Halleux, A. Köhler, A. El-Garoughy, E. W. Meijer, J. Barberá, J. Tant, J. Levin, M. Lehmann, J. Gierschner, J. Cornil and Y. H. Geerts, *J. Phys. Chem. B*, 2006, **110**, 7653–7659; (*h*) M. Lehmann, G. Kestemont, R. G. Aspe, C. Buess-Herman, M. H. J. Koch, M. G. Debije, J. Piris, M. P. de Haas, J. M. Warman, M. D. Watson, V. Lemaur, J. Cornil, Y. H. Geerts, R. Gearba and D. A. Ivanov, *Chem.–Eur. J.*, 2005, **11**, 3349–3362; (*i*) V. de Halleux, J. P. Calbert, P. Brocorens, J. Cornil, J. P. Declercq, J. L. Brédas and Y. Geerts, *Adv. Funct. Mater.*, 2004, **14**, 649–659; (*j*) L. Schmidt-Mende, A. Fechtenkötter, K. Müllen, E. Moons, R. H. Friend and J. D. MacKenzie, *Science*, 2001, **293**, 1119–1122.

12 M. Gharbia, A. Gharbi, H. T. Nguyen and J. Malthête, *Curr. Opin. Colloid Interface Sci.*, 2002, **7**, 312–325.

13 (*a*) V. N. Kozhevnikov, B. Donnio and D. W. Bruce, *Angew. Chem., Int. Ed.*, 2008, **47**, 6286–6289; (*b*) Y. Sagara and T. Kato, *Angew. Chem., Int. Ed.*, 2008, **47**, 5175–5178; (*c*) Y. Sagara and T. Kato, *Angew. Chem., Int. Ed.*, 2011, **50**, 9128–9132.

14 (*a*) B. P. Hoag and D. L. Gin, *Adv. Mater.*, 1998, **10**, 1546–1551; (*b*) T. Yasuda, K. Kishimoto and T. Kato, *Chem. Commun.*, 2006, 3399–3401; (*c*) T. Yasuda, H. Ooi, J. Morita, Y. Akama, K. Minoura, M. Funahashi, T. Shimomura and T. Kato, *Adv. Funct. Mater.*, 2009, **19**, 411–419; (*d*) Y. Sagara, S. Yamane, T. Mutai, K. Araki and T. Kato, *Adv. Funct. Mater.*, 2009, **19**, 1869–1875.

15 A. Pérez, J. L. Serrano, T. Sierra, A. Ballesteros, D. de Saá and J. Barluenga, *J. Am. Chem. Soc.*, 2011, **133**, 8110–8113; Compound **C_3B9** appeared as CA9 in this reference. Nomenclature has been modified in the present paper in order to make it coherent.

16 J. Barluenga, D. de Sáa, A. Gómez, A. Ballesteros, J. Santamaría, A. de Prado, M. Tomás and A. L. Suárez-Sobrino, *Angew. Chem., Int. Ed.*, 2008, **47**, 6225–6228.

17 (*a*) C. Lin, H. Ringsdorf, M. Ebert, R. Kleppinger and J. H. Wendorff, *Liq. Cryst.*, 1989, **5**, 1841–1847; (*b*) G. Staufer and G. Lattermann, *Makromol. Chem.*, 1991, **192**, 2421–2431; (*c*) J. Barbera, L. Puig, J. L. Serrano and T. Sierra, *Chem. Mater.*, 2004, **16**, 3308–3317.

18 (*a*) V. S. K. Balagurusamy, G. Ungar, V. Percec and G. Johansson, *J. Am. Chem. Soc.*, 1997, **119**, 1539–1555; (*b*) V. Percec, C. H. Ahn, W. D. Cho, A. M. Jamieson, J. Kim, T. Leman, M. Schmidt, M. Gerle, M. Moller, S. A. Prokhorova, S. S. Sheiko, S. Z. D. Cheng, A. Zhang, G. Ungar and D. J. P. Yeardley, *J. Am. Chem. Soc.*, 1998, **120**, 8619–8631; (*c*) V. Percec, W. D. Cho, P. E. Mosier, G. Ungar and D. J. P. Yeardley, *J. Am. Chem. Soc.*, 1998, **120**, 11061–11070.

19 In contrast to our results, the mesomorphic behavior of **B6** was described as cubic in ref. 18b. However, the structural parameters of the cubic mesophase were not reported therein.

20 (*a*) M. Kölbel, T. Beyersdorff, X. H. Cheng, C. Tschierske, J. Kain and S. Diele, *J. Am. Chem. Soc.*, 2001, **123**, 6809–6818; (*b*) T. Yatabe, Y. Suzuki and Y. Kawanishi, *J. Mater. Chem.*, 2008, **18**, 4468–4477.

21 B. M. Rosen, C. J. Wilson, D. A. Wilson, M. Peterca, M. R. Imam and V. Percec, *Chem. Rev.*, 2009, **109**, 6275–6540.

22 (*a*) E. Cavero, S. Uriel, P. Romero, J. L. Serrano and R. Giménez, *J. Am. Chem. Soc.*, 2007, **129**, 11608–11618; (*b*) H. Zheng, B. Xu and T. M. Swager, *Chem. Mater.*, 1996, **8**, 907–911; (*c*) H. Zheng, P. J. Carroll and T. M. Swager, *Liq. Cryst.*, 1993, **14**, 1421–1429; (*d*) H. Metersdorf and H. Ringsdorf, *Liq. Cryst.*, 1989, **5**, 1757–1772.

23 (*a*) G. Ungar, D. Abramic, V. Percec and J. A. Heck, *Liq. Cryst.*, 1996, **21**, 73–86; (*b*) V. Percec, C.-H. Ahn, T. K. Bera, G. Ungar and D. J. P. Yeardley, *Chem.–Eur. J.*, 1999, **5**, 1070–1083; (*c*) V. Percec, T. K. Bera, M. Glodde, Q. Y. Fu, V. S. K. Balagurusamy and P. A. Heiney, *Chem.–Eur. J.*, 2003, **9**, 921–935.

24 F. Vera, J. L. Serrano and T. Sierra, *Chem. Soc. Rev.*, 2009, **38**, 781–796.

25 J. Barberá, E. Cavero, M. Lehmann, J. L. Serrano, T. Sierra and J. T. Vázquez, *J. Am. Chem. Soc.*, 2003, **125**, 4527–4533.

26 J.-H. Ryu, L. Tang, E. Lee, H.-J. Kim and M. Lee, *Chem.–Eur. J.*, 2008, **14**, 871–881.

27 G. Gottarelli, S. Lena, S. Masiero, S. Pieraccini and G. P. Spada, *Chirality*, 2008, **20**, 471–485.

28 F. E. Eaton, *Pure Appl. Chem.*, 1988, **19**, 1107–1114.

29 J.-K. Fang, D.-L. An, K. Wakamatsu, T. Ishikawa, T. Iwanaga, S. Toyota, D. Matsuo, A. Orita and J. Otera, *Tetrahedron Lett.*, 2010, **51**, 917–920.

30 (*a*) M. O. Vysotsky, V. Böhmer, F. Würthner, C.-C. You and K. Rissanen, *Org. Lett.*, 2002, **4**, 2901–2904; (*b*) F. Wurthner, C. Thalacker, S. Diele and C. Tschierske, *Chem.–Eur. J.*, 2001, **7**, 2245–2253; (*c*) B. A. Gregg and R. A. Cormier, *J. Am. Chem. Soc.*, 2001, **123**, 7959–7960.

31 G. S. Pilzak, J. Baggerman, B. van Lagen, M. A. Posthumus, E. J. R. Sudhölter and H. Zuilhof, *Chem.–Eur. J.*, 2009, **15**, 2296–2304.

32 Z. Chen, U. Baumeister, C. Tschierske and F. Wurthner, *Chem.–Eur. J.*, 2007, **13**, 450–465.

33 F. Wurthner, Z. Chen, V. Dehm and V. Stepaneko, *Chem. Commun.*, 2006, 1188–1190.

34 (*a*) J. L. Brédas, R. Silbey, D. S. Boudreaux and R. R. Chance, *J. Am. Chem. Soc.*, 1983, **105**, 6555–6559; (*b*) S. Janietz, D. D. C. Bradley, M. Grell, C. Giebeler, M. Inbasekaran and E. P. Woo, *Appl. Phys. Lett.*, 1998, **73**, 2453–2455; (*c*) C. Chi and G. Wegner, *Macromol. Rapid Commun.*, 2005, **26**, 1532–1537; (*d*) J. del Barrio, L. S. Chinelatto Jr, J. L. Serrano, L. Oriol, M. Piñol and H. J. Bolink, *New J. Chem.*, 2010, **34**, 2785–2795.

35 E. Hendrickx, Y. Zhang, K. B. Ferrio, J. A. Herlocker, J. Anderson, N. R. Armstrong, E. A. Mash, A. P. Persoons, N. Peyghambarian and B. Kippelen, *J. Mater. Chem.*, 1999, **9**, 2251–2258.

36 G. Hernandez-Sosa, N. E. Coates, S. Valouch and D. Moses, *Adv. Funct. Mater.*, 2011, **21**, 927–931.

37 F. Vera, R. M. Tejedor, P. Romero, J. Barberá, M. B. Ros, J. L. Serrano and T. Sierra, *Angew. Chem., Int. Ed.*, 2007, **46**, 1873–1877.

